UiT The Arctic University of Norway

Faculty of Biosciences, Fisheries and Economics, Department of Arctic and Marine Biology

Interannual variability (2014-2019) of hydrography, fluorescence and nutrient distribution in Vestfjorden, Lofoten.

Daniel Fernández Román

BIO-3950 Master's thesis in Marine Ecology (May 2020)

Acknowledgements:

First of all, I would like to thank to my two amazing supervisors Angelika and Ingrid. I was really lucky to be able to work with you two, both in the cruise and during your supervision over the development of this exciting study to me. It was a very fun and enriching process. Thanks for all the patience, hard work and the skype meetings during the Corona times. Working on my master thesis helped me to grow as a researcher but also as a person, and that is thanks to you two.

I would like to thank also to Svein Kristiansen and Hans Christian Eilertsen for providing me with the nutrient data from (2015-2018) and to Jofrid Skarðhamar for sharing with me the freshwater runoff data from Vestfjorden. Thanks to the crew of R/V Helmer Hansen and to all the professors and students involved in the courses BIO-2010 Marine Ecology and BIO-2516 Ocean Climate from 2014-2019.

And of course I cannot forget about my family and friends who helped and supported me during my two years of master. Thanks to my dad, Alejandro for inspiring me and give me his scientific curiosity and to my mum, Susana, for teaching me to never surrender. Thanks to my friends that made these two years in Tromsø truly unforgettable. Thanks to the Svalbard crew for an amazing month up north, to Theo for your great friendship and the endless ski-trips / photo tours/ hiking / camping / sailing / fishing. To Alex for all the talks and ski trips we shared and for being the first person I met here in Tromsø when I came in firstly in 2017. Og takk til Siva, for alle opplevelsene sammen og at du va en skikkelig pro nosk lærer til mæ. I cannot mention all of you but this applies to everyone, it has been great to share these two years with all of you guys! And of course also my friends back home, thanks to the Cinderelic Olympic Team (Miguel, Marto and Pelos) for more than twenty years of friendship, to Olatz for your endless counselling and to everyone there that supported me in the last two years.

To all of you, THANK YOU!

Daniel Fernández Román,
Tromsø, June 2020.

Abstract

Vestfjorden is an area of great ecological relevance since it is one of the main spawning areas of North East Atlantic cod. The survival rate of the cod larvae depends greatly on the abundance of zooplankton, which in turn depends on phytoplankton. Due to the extreme seasonality of high latitude fjords with a short productive season, understanding the phytoplankton distribution in spring is crucial. Phytoplankton is greatly affected by hydrography and nutrient distribution. This study aims to identify a common pattern in hydrography, nutrient concentration and phytoplankton distribution in Vestfjorden and the impact of hydrography on phytoplankton distribution. To do that, hydrographic variables (T, S, ρ), nutrient concentration and fluorescence were sampled in different surveys in spring from 2014 to 2019. The results showed that Vestfjorden was stratified throughout spring in all years. In Spring, the surface layer was colder (3.0 – 4.0 ºC) and fresher (32.6 – 33.9 g/kg), than the bottom layer (7.0 – 7.5 ºC) and (> 34.9 g/kg). The formation of hydrographic features such as fronts or eddies were observed in the middle of the fjord. The phytoplankton distribution was linked to hydrography, especially to the presence of hydrographic features. The spring bloom may be triggered in the middle of the fjord, linked to the front/eddy, due to the suppression of vertical mixing. If not such structure is developed, the onset of the bloom may be delayed.

Keywords: Spring bloom, phytoplankton, eddy, front, stratification, Vestfjorden, hydrographic feature

Table of Contents

List of Tables

List of Figures

1 Introduction:

The Lofoten-Vesterålen shelf (including Vestfjorden), on the coast of Northern Norway, is highly ecologically relevant because is one of the biggest spawning areas for North East Atlantic cod (*Gadus morhua*; Ottersen *et al.*, 2014). Cod represents one of the most common commercially exploited fish stocks (Ottersen *et al.*, 2014) and has a big importance for Norwegian fisheries. The survival rate of cod larvae is affected to a large degree by hydrography and the abundance of *Calanus* sp. in spring (Ellertsen *et al.*, 1987). At the same time, *Calanus* sp. availability is influenced by hydrography as well as phytoplankton abundance (Cushing, 1990; Degerlund & Eilertsen, 2010). The match-mismatch theory (Cushing, 1990) explains how the spring bloom is important on regulating the abundance of *Calanus* sp. population, which later will feed the cod larvae.

Vestfjorden is influenced by two main water masses, Norwegian Coastal Water (NCW) and Atlantic Water (AW) (Furnes and Sundby, 1981), and two currents, the Norwegian Coastal Current (NCC) and the Norwegian Atlantic Current (NCC) (Sætre, 1999; Mitchelson and Sundby, 2001). There are three different layers in the fjord; the NCW is on the surface (50 – 150 m), followed by a thermocline and the AW (Furnes and Sundby, 1981). The surface layer varies seasonally whereas the bottom layer is more stable throughout the year (Furnes and Sundby, 1981). Vestfjorden has a deep sill (~ 300 m) and a wide mouth (~ 70 km), it therefore is not a fjord by traditional definition, but more similar to a coastal bay surrounded by real fjords (Mitchelson & Sundby, 2001). Due to this, the fjord presents a complex circulation pattern (Espinasse *et al.*, 2016) and a considerable exchange with the shelf. Apart from the classic estuarine circulation in fjords (Cottier *et al.*, 2010; section 2.1), Vestfjorden is affected by the rotation of the earth. Thus, the major inflow of shelf waters enters the fjord in the east, close to the mainland, and the outflow on the west, near Lofoten islands (Eggvin, 1931; Sundby, 1978; Furnes and Sundby, 1981).

The interactions between the Norwegian Coastal Current (NCC) and the Norwegian Atlantic Current (NAC), the wind (Jones *et al.*, 1997) and the presence of hydrographic different features (fronts and eddies; Mitchelson and Sundby, 2001) will influence the hydrography and the circulation in Vestfjorden. The appearance of hydrographic features like eddies or fronts in the fjord is common (Mitchelson & Sundby, 2001) and varies interannually and on short time scales, depending on hydrographical and meteorological conditions.

Hydrography in general (stratification, water mass distribution) and the hydrographic features (eddies and fronts; Mahadevan, 2016) affect the distribution of phytoplankton in the ocean (section 2.4 and 2.5). Therefore, it is necessary to study these processes in Vestfjorden to understand how they affect to the phytoplankton in the fjord.

This study aims to find common patterns in the hydrography and nutrient concentrations in Vestfjorden as well as the hydrographic features that might appear in the fjord. Hydrographic variables measured along the same transect in spring 2014 to 2019 are analysed to discuss interannual and short-term variability in the fjord, taking into account environmental parameters such as wind, precipitation and river runoff. In a second step it is investigated how the abiotic conditions can be related to the fluorescence, which is used here as a proxy for phytoplankton biomass.

In this study I (1) look for a general pattern in the hydrography in the fjord, as well as its interannual variability and the presence of hydrographic features, (2) analyse the distribution and interannual variability of fluorescence and nutrient concentrations, and (3) try to answer if hydrography and nutrient concentrations have an effect on the fluorescence distribution in Vestfjorden.

The thesis is organised as follows: a theoretical background section in which I will explain with more detail oceanographic terms and concepts that might be necessary to understand the study, a wider representation of the circulation in Vestfjorden and an insight of the spring bloom. This chapter is followed by a results part where the main findings will be highlighted and a discussion part in which the results will be discussed and the research question will be answered.

2 Theoretical background

2.1 Physical processes in a fjord

Fjords are characteristic marine environments which act as the link of land and ocean and create a marine environment of great ecological value (Cottier *et al*., 2010). Fjords were formed by glacier activity and they present different oceanographic and geographical conditions, e.g., wide or narrow fjords, with sill or without, ice-covered or ice free (Syvitski *et al*., 1987). The oceanographical conditions of fjords provide a pseudo-mesocosm to study different biological parameters, among them, life histories, abiotic-biotic coupling or trophic linkages (Cottier *et al.*, 2010). Fjords are widely distributed in the world, and since they were formed by glacial carving, they are located in mid to high latitudes, i.e., above 45º N/S (Farmer and Freeland, 1983). Although there is the concept of a "typical" fjord, such a wide range will affect their characteristics (Inall and Gillibrand, 2010).

The most common water mass distribution in fjords is a three-layer system (Farmer and Freeland, 1983; Cottier *et al.*, 2010). This is represented by a fresh surface layer, an intermediate advected water layer and a deep winter water layer. Although this is a common pattern, the water mass distribution in a fjord varies a lot through seasons and geographically (Farmer and Freeland, 1983). In high latitude fjords, this concept is for example only fully applying in summer (Svendsen *et al.*, 2002; Cottier *et al.*, 2010). Unlike coastal areas in which the seasonal vertical density distribution is governed by solar driven thermal stratification, fjords vertical density distribution is most often ruled by salinity (Inall and Gillibrand, 2010). This is due to flow restrictions and high freshwater input, and in mid latitude fjords these processes show no clear seasonal pattern. In comparison, high latitude fjords present a high seasonality in their water layering distribution due to the high seasonality of the freshwater runoff and the inflow of the different water masses (Cottier *et al*., 2010).

The seasonal cycle in high latitude fjords, is as follows (Cottier *et al.*, 2010):

- In summer, the surface is fully stratified, and when ice-free, wind mixing will dominate.
- In autumn, due to the increase of winds, there is a loss of sensible heat from the fjord to the atmosphere, and therefore a decrease of the water temperature, and thus a deepening of the mixed layer (Cottier *et al.*, 2007). The remaining mixed water mass is defined as Local Water (Svendsen *et al.*, 2002; Nilsen *et al.*, 2008; Cottier *et al.*, 2010).

- In winter, when the water reaches the freezing point, sea ice starts to form, thus releasing brine and fully mixing the water column.
- In spring, after the ice break up, the surface temperature increases due to heating and salinity decreases due to freshwater input when the melting period starts. Therefore, re-stablishing the strong pycnocline and eventually leading to summer conditions.

Although in Vestfjorden there is not sea-ice covered in winter, this fjord presents also a high seasonality therefore staying in between of a high latitude fjord and a mid latitude fjord.

Stratification in a fjord is determined by freshwater input, surface heat fluxes, and baroclinic exchanges (Inall and Gillibrand, 2010). Freshwater supply in fjords is high, both by riverine input (Inall and Gillibrand, 2010) and snowmelt (Cottier *et al.*, 2010). Deep water renewal by baroclinic processes can lead in to changes in stratification (Inall and Gillibrand, 2010).

Both mid latitude fjords and high latitude fjords present external forcing that mix or modify water masses, and determine the extent of both horizontal and vertical circulation of water masses within the fjord (Inall and Gillibrand, 2010; Cottier *et al.*, 2010). Most of these modifications depend on the vertical mixing and advection of other water masses into the fjord (Cottier *et al.*, 2010). The exchange of water masses and circulation in fjords is controlled by barotropic and baroclinic exchanges (Inall and Gillibrand, 2010). A barotropic flow is the one which is driven by variations in the surface height of the ocean. In a fjord, the barotropic exchanges are caused by tides, storm surges and mean sea level change (Inall and Gillibrand, 2010).

Baroclinic flows are caused by the differences in vertical density distribution between two different locations. These differences in density and thus stratification generate pressure gradient forces which vary with depth, thus producing flows which vary also with depth (Inall and Gillibrand, 2010). The most common baroclinic flow, and therefore the main circulation pattern in fjords is the estuarine circulation (Inall and Gillibrand, 2010; Cottier *et al.*, 2010). As explained in the review by Inall and Gillibrand (2010), in a fjord during an averaged tidal cycle, fresh water will flow out of the fjord while more saline water will flow into the fjord in the deeper layer. At the boundary between the two layers, the shear between the two currents (surface inflow / deep outflow) will induce mixing. Thus, a horizontal gradient in the hydrographic properties (T, S and ρ) from the head to the mouth of the fjord can form as the surface layer is slightly mixed with the bottom layer.

The classic estuarine circulation (and other baroclinic processes) can be affected by the rotation of the earth (Inall and Gillibrand, 2010; Cottier *et al.*, 2010). The importance of the rotational effects on the circulation of a fjord can be assessed with the internal Rossby radius (Inall and Gillibrand, 2010; Cottier *et al.*, 2010). This is a ratio between the speed of the internal wave (dependent on stratification) and the Coriolis parameter (*f*). Thus, the Rossby radius is a balance of the importance of the relative importance of stratification and the rotation (Cottier *et al.*, 2010). The Rossby radius r_i is given by (taken from Cottier *et al.*, 2010):

$$r_i = \frac{c_i}{f} \tag{1a}$$

where

$$c_i^2 = \frac{g' H_1 H_2}{H} \tag{1b}$$

is the speed of an internal wave and

$$g' = g\,\frac{(\rho_2 - \rho_1)}{\rho_2} \tag{1c}$$

is the reduced gravity with ρ_1 and ρ_2, and H_1, H_2 being the densities and depths of the upper and lower layer, respectively. H represents the total water depth and f the Coriolis parameter. If the internal Rossby radius is smaller than the width of the fjord, the circulation of it will be affected by the rotation of the earth. This effect causes the deflection of baroclinic flows such us, estuarine circulation or intermediate exchange flows, to the right (left) in the northern (southern) hemisphere (Inall and Gillibrand, 2010). In Vestfjorden, r_i is smaller than the width of the fjord (see Section 4.2.3), thus rotational effects are important on the physical processes in the fjord.

Wind is key to understand the processes of vertical mixing and circulation (Cottier *et al.*, 2010) and the topography of the land can affect the strength and variability by the steering of the winds (Jones *et al.*, 1997; Skogseth *et al.*, 2007; Inall and Gillibrand, 2010; Cottier *et al.*, 2010). Due to the steering, the winds in fjords are usually bimodal, that means, either down-fjord or up-fjord (Cottier *et al.*, 2010). Wind-driven circulation can also cause a baroclinic flow which has a great importance in fjords due to their shallow freshwater layer (Inall and Gillibrand, 2010). The main effects of wind in a fjord are modifying the outflow of surface brackish water

(both decreasing it and intensifying it; Skogseth *et al.,* 2007; Cottier *et al.,* 2010) and generating upwelling (Cottier *et al.,* 2010). Wind is able to push the surface water masses along the fjord. Sustained up-fjord winds can pile up the freshwater at the head of the fjord, reversing the surface brackish flow (Cottier *et al.,* 2010), thus producing a downward slope in the pycnocline towards the head of the fjord and inducing an opposite direction flow in the layer underneath (Inall and Gillibrand, 2010). Down-fjord winds will intensify the outflow of brackish water to the right hand of the fjord (in the north hemisphere) (Cottier *et al.,* 2010). This will be further reinforced by the Ekman transport to the right of the wind, generating a cross-fjord pressure gradient (Svendsen *et al.,* 2002; Cottier *et al.,* 2010) which will maintain the enhancement of the outflow after the wind is relaxed (Ingvaldsen *et al.,* 2001; Cottier *et al.,* 2010). Rapid changes in wind direction can reverse the circulation of the fjord in short time scales (Skarðhamar and Svendsen, 2010). Skarðhamar and Svendsen (2010) showed that, within a timescale of 1 day, a change from weak down-fjord winds to stronger up-fjord winds produced a reversal in the horizontal surface temperature and salinity gradient, a reduction of stratification, and thus an increase in vertical mixing.

The circulation in and out of the fjords make them a link between the terrestrial domain and the oceanic domain (Cottier *et al.,* 2010). Usually, a strong boundary current flowing alongside the shelf slope, bring the oceanic water masses to the shelf allowing the exchange between the shelf and the fjord (Cottier *et al.,* 2010). For fjords without a sill as for example Kongsfjorden, Svalbard (Cottier *et al.,* 2007), the interaction between shelves and the boundary current are key for controlling the exchange. Eddies in the front between the boundary current and the shelf water are one of the most important mechanisms ruling the cross-shelf exchanges (Nilsen *et al.,* 2006; Cottier *et al.,* 2010), and the upwelling of the bottom boundary current (Cottier *et al.,* 2007; Cottier *et al.,* 2010). The inflow of water masses at mid-depth into the fjord is associated with the enhancement of the estuarine circulation by wind forcing (Cottier *et al.,* 2007; Cottier *et al.,* 2010), inducing then a compensating flow from the shelf (Nilsen *et al.,* 2008; Cottier *et al.,* 2010). Usually, in fjords without a shallow sill, fjord-shelf exchange is controlled by the boundary current flowing along the mouth of the fjord, controlling the entrance of shelf surface and intermediate waters into the fjord (Cottier *et al.,* 2010). This process has been defined as "geostrophic control" by (Klinck *et al.,* 1981). The degree of control is determined by the strength of stratification the coastal waters and the intensity of the along shelf winds (Cottier *et al.,* 2010). The stronger the coastal boundary current, the lesser the exchange between shelf and fjord.

2.2 The physical environment of Vestfjorden

The two main water masses influencing Vestfjorden are the Atlantic Water (AW) and Norwegian Coastal Water (NCW). The sill of Vestfjorden (> 300 m) reduces the exchange of deep waters therefore suffering little variation in its water mass properties. Following Furnes and Sundby, (1981), there are three layers and two water masses in Vestfjorden: In winter, there is a surface layer (i.e., NCW) with temperature from 2 – 4 ºC, and a salinity of 33-34 kg m^{-3}. The thickness of this layer varies from 50 to 150 m. During the transition from winter to summer, this layer warms up due to increase of air temperature and solar heating and freshens due to the increase freshwater runoff (Sundby, 1978). Below the surface layer, there is a deep water layer of Atlantic origin, temperatures ranging from 6.5 – 7 ºC and salinity of 34.7 – 35 kg m^{-3}. In between these two water masses there is a thermocline of thickness ranging between 10 – 50 m (Sundby, 1978; Furnes and Sundby, 1981). The thickness of the thermocline depends greatly on meteorological processes. During high precipitation winters, the thermocline can extend over 200 m whereas in dry and cold winters it can be up to 50 m (Mitchelson and Sundby, 2001). This displacement of water masses is stronger at the head of the fjord, and from the sill outwards it disappears, increasing the density rather constant from surface to bottom (Furnes and Sundby, 1981; Mitchelson and Sundby, 2001).

Vestfjorden has a complex circulation pattern dominated mainly by the Norwegian Coastal Current (NCC, figure 1) and the Norwegian Atlantic Current (NAC, figure 1). The NCC originates in the south of Norway from mixing of Norwegian Coastal Water (formed by outflow from the Baltic Sea and the freshwater runoff of Norway) with North Sea Water and Atlantic Water (Sætre, 1999). The NCC flows northward along the coast forming a characteristic low salinity wedge (< 35 g kg^{-1}; Sætre, 1999; Mitchelson & Sundby, 2001; Albretsen *et al.,* 2012; Espinasse *et al.,* 2016). Salinity and temperature of the NCC change from its formation along the Norwegian coast (Sætre, 2007; Albretsen *et al.,* 2012). South of Vestfjorden, the NCC divides in two main branches, one going to the west around the Lofoten archipelago and continuing northwards close to the coast, and the other going north into Vestfjorden and playing an important role for the circulation pattern inside Vestfjorden (Espinasse *et al.,* 2016). The percentage of the total volume of the NCC entering Vestfjorden is around 10 % (Sundby, 1978).

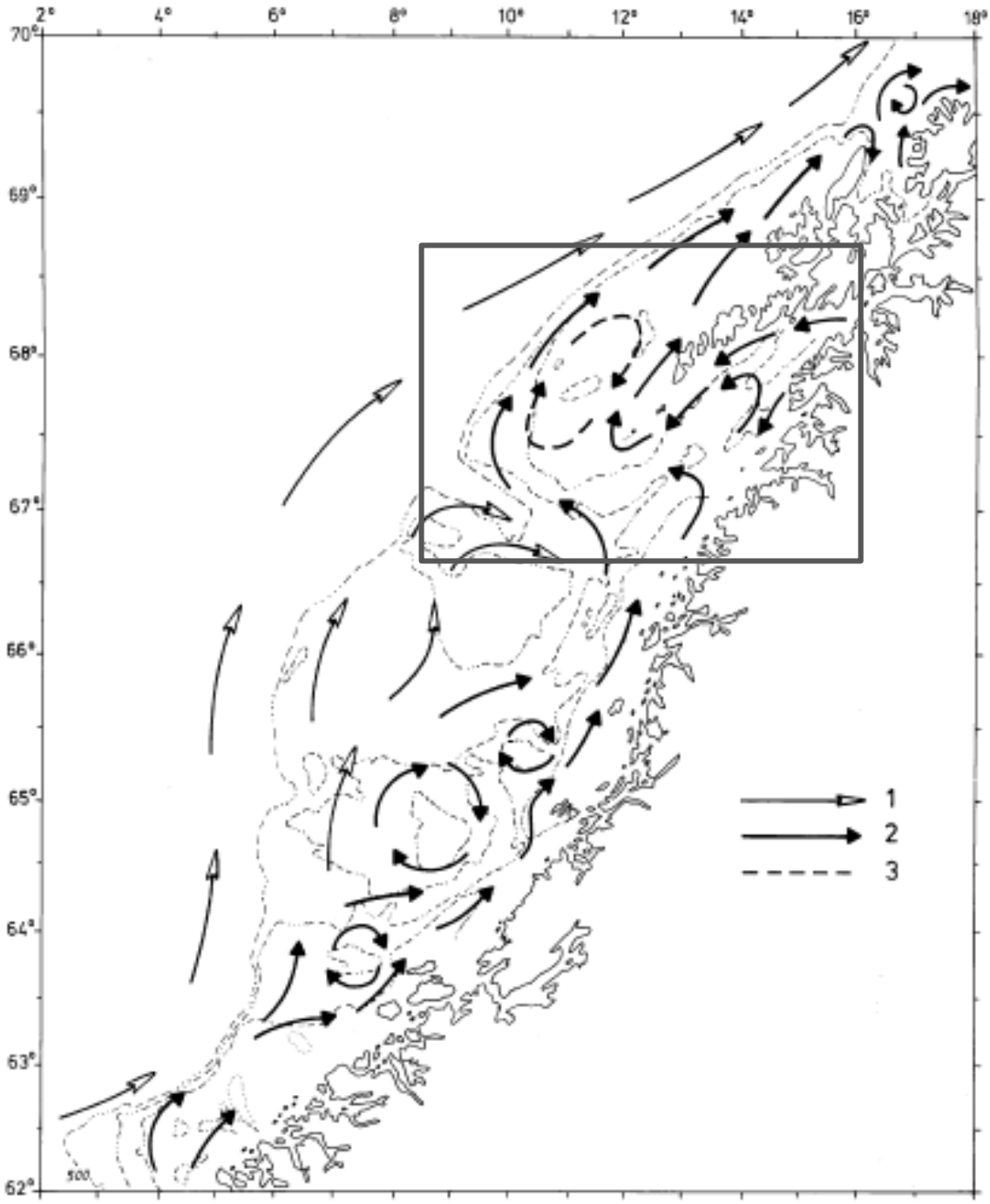

Figure 1 Upper water column currents along the Norwegian coast. Vestfjorden is located in the grey box. Figure adapted from figure 2 in Sætre, (1999). (Original from Sætre, 1983).

The NAC is a continuation of the Gulf Stream that flows northwards close to the continental slope (Helland-Hansen & Nansen, 1909) with a typical high salinity signal (~35%). The interaction of the NAC and NCC is important to control the amount of AW that enters Vestfjorden by cross-shelf exchange (Espinasse *et al.,* 2016). Entrance of AW from the shelf is noted to be an important process in terms of biology. Espinasse *et al.,* (2016) found that

zooplankton is advected in to Vestfjorden, and thus also phytoplankton may be advected, which could be relevant for the present study.

The main circulation pattern in Vestfjorden consists in an inflow current on the east side (mainland) and one outflow current on the west side (Lofoten archipelago; Eggvin, 1931; Sundby, 1974). Although this is the most frequent circulation pattern, circulation inside Vestfjorden is influenced by wind action and tidal forcing. High mountains on the Lofoten archipelago and the mainland cause a steering of the prevailing winds (Jones *et al.,* 1997) which impacts the surface circulation in the fjord (see also section 2.1). In periods with winds coming from the south west (SW winds, up-fjord), there is upwelling on the Lofoten side of the fjord (Furnes and Sundby, 1981). With periods of north east winds (NE winds, down-fjord), the circulation in Vestfjorden is observed to be reversed leading to downwelling along Lofoten (Mitchelson and Sundby, 2001).

Apart from this main circulation pattern, the appearance of mesoscale features likes eddies or fronts in the fjord is common (Mitchelson & Sundby, 2001). The most common location for an eddy is in central Vestfjorden, but some smaller eddies can be found in the inner fjord west of Røst (Mitchelson & Sundby, 2001). As Mitchelson & Sundby (2001) showed, there is a semi-permanent anticyclonic eddy in central Vestfjorden which forms in late spring and remains present throughout periods of stable atmospheric conditions. In the case of Vestfjorden, the formation of the eddy is driven by the baroclinic currents associated with the front (Mitchelson and Sundby, 2001). The smaller eddies are largely affected by the prevailing winds, determining the direction of the eddy rotation. The restrictions on the flow on both NCC and freshwater input will determine the position of the mesoscale features (Mitchelson & Sundby, 2001).

2.3 Role of nutrients in the ocean. Northern Norway nutrient distribution.

Nutrients and light are the most important drivers of phytoplankton growth. The nutrient concentration varies a lot seasonally and geographically. Photosynthetically available light decreases exponentially in the water column, supporting photosynthesis only in the euphotic zone (<100 m). Thus, the nutrient concentration increases with depth at the same time that phytoplankton growth decreases. To grow, phytoplankton takes up nutrients in an average ratio of 106 C: 16 N: 1 P: 0.0075 Fe (Carbon, nitrogen, phosphorus and iron) what is known as the Redfield ratio (Bristow *et al.*, 2017). The sources of P, Si, and Fe in the ocean are basically

limited to atmospheric and/or land/river input (Bristow *et al.*, 2017). In the case of nitrogen, apart from these sources there is the biological fixation of molecular nitrogen (N_2). This study is focusing in the most common use nutrients, the macronutrients (N, P and Si). For each I focus in the most common chemical specie for each element, nitrate (NO_3^-) and nitrite (NO_2^-) for nitrogen, silicate ($SiOH_4$) for silica, and phosphate (PO_4) for phosphorus (Stedmon, personal communication). Concentrations of nitrate usually are double the phosphate concentrations (Eilertsen and Taasen, 1984) and the concentration of silicate is similar to nitrate (Bech, 1982; in Eilertsen and Taasen, 1984).

At high latitudes, due to the seasonality of light and stratification, the phytoplankton growth period presents also a strong seasonality (Eilertsen and Taasen, 1984; Eilertsen and Frantzen, 2007). The nutrient concentration is linked to the phytoplankton growth, decreasing by the usage by the primary producers. Therefore, in layers with elevated phytoplankton growth (i.e., euphotic layer) the nutrient concentration will decrease until it is depleted (if there are no additional sources of nutrients). During winter the surface is nutrient rich but the low light regime limits the phytoplankton production and growth. Once the light stops to be limiting in spring, the growth of phytoplankton starts and therefore a strong decrease on nutrient concentration occurs within the euphotic layer (Hung Peng *et al.*, 1987; Takahashi *et al.*, 1993). The establishing of a strong pycnocline in spring/summer (Cottier *et al.*, 2010), makes the exchange of nutrients with the nutrient rich bottom layer very small. This, added to the high phytoplankton growth, makes the surface layer to be nutrient depleted (Hung Peng *et al.*, 1987). Since below the euphotic depth the phytoplankton growth is near zero, the nutrient concentration it is very high. During autumn, convective mixing and more frequent storms weaken the water column stratification and replenish the nutrient concentration in the surface water masses by mixing them with deep nutrient-rich waters.

There are not many surveys that studied the variations in nutrient concentration along the Northern Norway coast. Eilertsen and Taasen (1984) studied the seasonal nutrient dynamics from 1976 – 1978 in Balsfjorden. The main seasonal pattern was similar to the explained before. However, the onset of the spring bloom in Balsfjorden took place in a fairly homogenous water column, having then a rather constant nutrient concentration within the water column. At the end of the exponential growth phase of the bloom, the nitrate minimum was reached before than the phosphate minimum.

In Vestfjorden, the main source of nutrient comes from Atlantic Waters and the Norwegian Coastal Current (NCC) (Sætre, 2007). Coastal waters (from the NCC) have lower nutrient concentration than the Atlantic water. Sometimes in summer there is a subsurface nutrient maximum due to the intrusion of Atlantic Water (Sætre, 2007). Advection of nutrients into the fjord plays an important role on the distribution of nutrients in Vestfjorden.

Therefore, the study of the surface nutrient concentration in the fjord will give an insight into the phase of the spring bloom.

2.4 Interaction between hydrographic features and phytoplankton growth

The stratification allows phytoplankton to stay in the euphotic layer, whereas the mixing, will facilitate to replenish the surface layer with nutrients. Thus, the physical processes in the upper layer impact the phytoplankton production (Mahadevan, 2016). Nutrient distribution, dynamical conditions, light regime and growth, will control the way of how different hydrographic features will affect production (Mahadevan, 2016). Some hydrographic features, as eddies or fronts, will be very important in nutrient depleted regions (Mahadevan, 2016) (e.g., Vestfjorden during the spring bloom), allowing the replenishment of nutrients from deeper nutrient-rich water masses. In light-limited areas, (e.g., Vestfjorden prior the spring bloom), eddies can alter the mixed layer stratification by the generation of shallow mixed layers exposing the phytoplankton cells to light, triggering the spring bloom (Mahadevan *et al.,* 2010; Mahadevan, 2016).

The present study will focus in two different hydrographic features observed in Vestfjorden: Oceanic fronts and eddies. An oceanic front forms when there is a horizontal gradient of T, S or density in the ocean that is maintained within the mixed layer. A front can be detected in a section plot by the vertical pilling of the isolines (T, S, ρ). Fronts in the mixed layer are very susceptible to baroclinic instability (Boccaletti *et al.,* 2007) leading to the formation of mixed layer eddies. In contrast to fronts, eddies within the mixed layer produce the slumping of the isopycnals, thus restratifying the mixed layer. Also, the uplifting of the isopycnals by the eddies, can allow the entrance of nutrients from deeper layers (Siegel *et al.,* 1999; Mahadevan, 2016). As well, the vertical circulation typical of the fronts, supports the vertical advection of nutrients from deeper layers (Mahadevan and Archer, 2000; Mahadevan, 2016).

The presence of hydrographic features in Vestfjorden is discussed in the previous section (section 2.3). Knowing that Vestfjorden presents a multitude of hydrographic features, it is fair to think that they might affect to the nutrient availability and thus the phytoplankton growth in the fjord.

2.5 The spring bloom.

The rapid increase of phytoplankton abundance in spring is defined as the spring bloom. The spring bloom is a critical food source for the upper trophic levels in the food web (Cushing, 1990; Smayda, 1997). During the development of the bloom, there are three points that can be defined (Llort *et al.*, 2015):

- Onset of the bloom: Defined as the point in which the biomass starts to accumulate
- Climax: After the bloom is triggered, and when there is not nutrient/light limitation the phytoplankton accumulates at a maximum rate. The climax is the point at which the phytoplankton accumulation rate is maximal. From this point phytoplankton will still be accumulated but a lower rate.
- Apex: Is the point at which the bloom has its maximum biomass. From this point on, the biomass of phytoplankton will start decreasing.

Due to the polar night, and therefore a high seasonality on light availability, the phytoplankton growth in northern latitudes (among them Northern Norway) present a great seasonality, being the productive season much shorter than further south (Eilertsen and Taasen, 1984; Eilertsen and Frantzen, 2007). In Northern Norway, phytoplankton concentrations remain very low in winter (Eilertsen and Dagerlund, 2010). During the transition through winter to spring, the, combination of different background conditions lead to the onset of the spring bloom and its posterior development.

As noted in the introduction, the mechanisms regulating the onset of the spring bloom are still unclear (Franks, 2014). The first theory proposed aiming to explain the onset of the spring bloom was the Critical Depth Theory (SCD) (Sverdrup, 1953). This theory was proposed based on the assumptions of Gran and Braarud (1935) which showed how the phytoplankton production was limited by the high turbidity and turbulence of the waters. Sverdrup (1953) stated that for phytoplankton growth to occur, the production of organic matter had to be bigger than the destruction of it. For that he assumed that the water column has a mixed layer (ML) of thickness D and that phytoplankton was evenly distributed within it. During the onset phase of

the bloom, he assumed that the phytoplankton growth was just light limited (and not nutrient limited) and the phytoplankton losses are defined by respiration and are constant with depth.

For explaining the bloom, Sverdrup (1953) defined the depths:

- Compensation Depth: It is the depth in which the production (at that depth) equals the respiration (at that depth).
- Critical Depth: It is the depth in which the integrated production (with time and depth) equals the integrated respiration (with time and depth) equation (2).

$$Z_{cr} \rightarrow \int_0^t \int_0^D dp\, dt = \int_0^t \int_0^D dr\, dt \qquad (2)$$

Based on these assumptions Sverdrup proposed that for the spring bloom to be triggered, the critical depth has to be deeper than the mixed layer depth (MLD), so the phytoplankton can stay within the surface water layer in which growth is positive.

Following SCD (Sverdrup, 1953) a lot of theories were proposed to try to explain new observations made regarding spring blooms. In the early 90s, some authors reported the presence of a spring bloom in not stratified waters (Townsend *et al.*, 1992; Eilertsen, 1993) which was going against the SCD theory. To explain that, Huisman *et al.*, (1999) proposed the Critical Turbulence Theory by relaxing the assumption from Sverdrup that the phytoplankton cells were evenly distributed within the water column. In their model, phytoplankton dynamics depended of phytoplankton growth and vertical turbulent mixing. If turbulent mixing was strong, the MLD had to be shallower than the critical depth since the phytoplankton would be evenly distributed within the water column and therefore have to stay in the euphotic zone. But if mixing is weak (low turbulence) the water column does not have to be stratified because phytoplankton will not be exposed to vertical mixing. From this theory there are many modifications having in common the quantification of turbulent mixing in terms of turbulent dissipation. The shut-down on turbulent mixing can be linked to end of convective forcing (heat fluxes from $Q < 0$ to $Q > 0$) (Taylor and Ferrari, 2011b), presence of oceanic fronts (Taylor and Ferrari, 2011a), eddy slumping restratification (Mahadevan *et al.*, 2012) and change from buoyancy mixing regime to wind driven regime (Brody and Lozier, 2014).

Breaking with SCD (Sverdrup, 1953), Behrenfeld (2010), proposed that yearly phytoplankton cycle was ruled by the decoupling between grazing and primary producers, and that the spring bloom started to develop in mid-winter the latest.

Trying to unify the proposed theories, Chiswell *et al.* (2015), proposed that the positive growth of phytoplankton started when the ocean transitioned from deep mixing regime to a low turbulence regime but that the maximum growth (i.e., spring bloom onset) was not happening until heat fluxes turn positive.

Nowadays there is not a unified theory that works for the world oceans that explain the interannual and spatial variability of the spring bloom (Franks, 2014; Cole *et al.,* 2015) and the proposed studies have to be taken with "healthy scepticism" since they are averaging variables that have a strong non-linear response and they are not taking in to account short scale processes. Therefore, since there is not a unified theory explaining the onset of the spring bloom, it is necessary to study each region, taking to account also the short scale processes.

Focusing in my study region, the initiation of the bloom in Northern Norway (among it Vestfjorden) remains unclear. The initiation of the bloom varies depending on the fjord (Eilertsen and Frantzen, 2007), being Vestfjorden one on the earliest fjords (end of March) in Northern Norway in which the bloom is triggered (Huseby, 2002). Spring bloom in northern areas is found to start prior the stratification of the water column (Eilertsen *et al.,* 1981; Eilertsen and Taasen, 1984; Eilertsen, 1993). Although, one of the latest surveys on the Spring Bloom signalled that the spring bloom onset in Vestfjorden happened with the onset of spring stratification (Huseby, 2002).

During the first phase of the bloom, before the climax, phytoplankton is accumulated in to the surface layer (Lutter *et al.,* 1989). At the peak of the bloom, in the fjords of Northern Norway, the biomass is maximum in the subsurface (c.a., 10 m) (Eilertsen and Taasen, 1984; Lutter, *et al.,* 1989). The subsurface maximum is typical in northern fjords (e.g., Balsfjorden) (Eilertsen and Taasen, 1984), being accumulated under the pycnocline due to the nutrient depletion in the surface layer (Lutter *et al.,* 1989). The termination of the bloom in Balsfjorden is caused by a combination of nitrate and phosphate depletion, shelf-shading effect of the phytoplankton cells and grazing pressure (Eilertsen and Taasen, 1984; Lutter *et al.,* 1989). The timing of the spring bloom in Vestfjorden was similar to the rest of the fjords of Northern Norway (Huseby, 2001).

With this information, this study aims to identify in which phase the spring bloom during the sampling is and which mechanisms could play a role during the development of the bloom.

3 Data and methods:

3.1 Data available:

The hydrographic, nutrient, and chlorophyll *a* data used for this thesis were collected during teaching cruises run by UiT The Arctic University of Norway (UiT) on board RV Helmer Hanssen. The teaching cruises took place annually in spring as part of the UiT courses BIO-2010 Marine Ecology and BIO-2516 Ocean Climate, and data were obtained for the period 2014-2019. Nutrient data for 2015-2018 were provided by Svein Kristiansen. In 2019, I participated in the BIO-2010/BIO-2516 teaching cruise and collected chlorophyll *a*, phaeophytin, and nutrient samples.

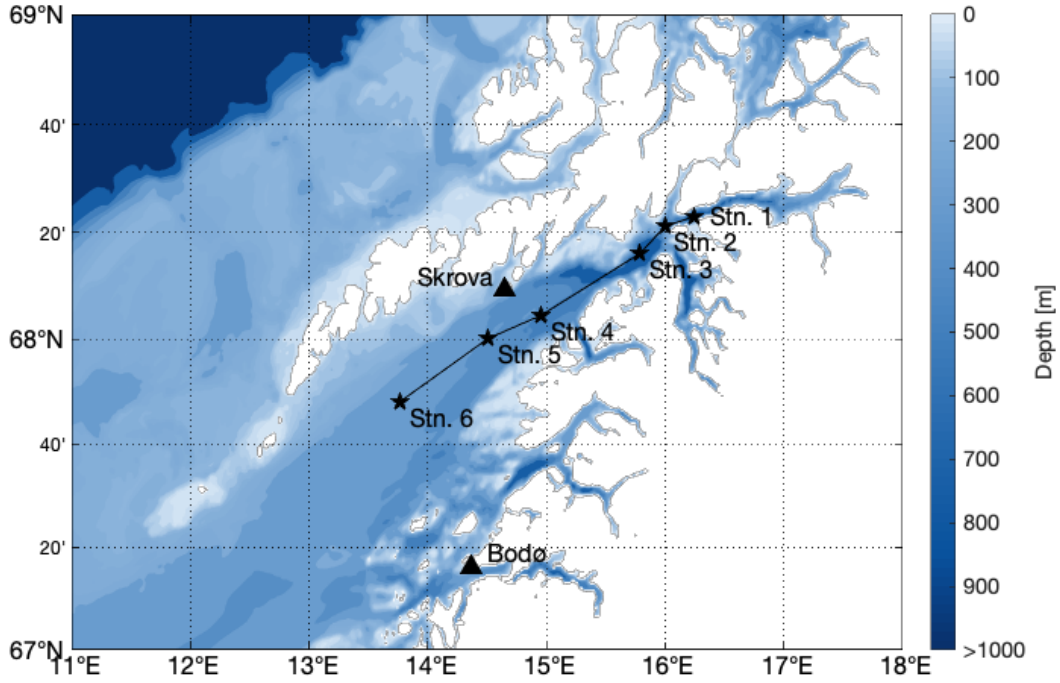

Figure 2 Map of the stations of the cruises. Stn 1, 2, 3, 4, 5 and 6 represent the place where the hydrographic and nutrient data was taken. Skrova is the meteorological station were wind data was obtained from. Bodø is the meteorological station were air temperature data was obtained from.

Table I All the transects taken during all the teaching cruises. The "x" means there is no data for that station. CTD means there are hydrography data (T, S, Density, Fluorescence) and nutrients that there are nutrient data (NO_3 + NO_2 , $SiOH_4$, PO_4).

Transect	Station 1	Station 2	Station 3	Station 4	Station 5	Station 6
2014 (23/04 to 24/04)	CTD	x	CTD	CTD	CTD	CTD
2015 (14/04 to 15/04)	CTD / Nutrients	CTD / Nutrients	CTD / Nutrients	CTD / Nutrients	CTD / Nutrients	CTD / Nutrients
2016 April I (01/04 to 02/04)	CTD / Nutrients	CTD / Nutrients	CTD / Nutrients	CTD / Nutrients	CTD / Nutrients	CTD / Nutrients
2016 April II (06/04 to 07/04)	CTD	CTD	CTD	CTD	CTD	CTD
2016 April III (10/04)	CTD	CTD	CTD	CTD / Nutrients	CTD	CTD / Nutrients
2017 March (29/03)	CTD / Nutrients	CTD / Nutrients	CTD / Nutrients	CTD / Nutrients	CTD / Nutrients	CTD / Nutrients
2017 April (23/04 to 24/04)	CTD	CTD	CTD	CTD	CTD	CTD
2018 (8/04 to 11/04)	CTD / Nutrients	CTD / Nutrients	CTD / Nutrients	CTD / Nutrients	CTD / Nutrients	CTD / Nutrients
2019 April I (05/04 to 06/04)	CTD	CTD	CTD	CTD	CTD	CTD
2019 April II (10/04)	x	CTD	CTD	CTD	x	x
2019 April III (13/04)	CTD	CTD	CTD	x	x	x

In the following, data from each cruise are named after the year (e.g., 2014) and the month in case the Vestfjorden transect was taken more than once that year. If several transects were taken during the same month, the different sampling times are in addition labelled with roman numbers (table I).

3.2 Hydrographic data:

To obtain vertical profiles of temperature, salinity, and fluorescence, a Conductivity – Temperature – Depth (CTD) probe was lowered through the water column to 10 m above the bottom. The CTD consisted of a Seabird Electronics (SBE) 911plus package with conductivity cell (SBE 4c, S/N 2666), temperature sensor (SBE 3plus, S/N 4497), pressure sensor (S/N 77984), dissolved oxygen (SBE 43, S/N 2557), a Seapoint fluorometer (S/N 3049) and turbidity meter (S/N 10894), and a Satlantic PAR sensor (S/N1060). Sensors were mounted in a rosette

with 12 niskin bottles of 5 L to take water samples. The CTD was controlled by the SBE Seasave software. GPS information (NMEA string) was added directly to the CTD files from the Seapath positioning system of the ship. Preliminary post-processing of the hydrographical data was carried out after each cast by using a SBE32 batch written by the UiT technicians (Hans Dybvik, Ronald Berntsen, John-Terje Eilertsen) which calls the SBE data processing routines provided in the SBE website. A finer calibration of the CTD data was made by using routines provided by my supervisor (Dr. Angelika Renner). First, the routine ctdcal.m, reads the ".cnv" files (output from the SBE software), renames all the variables in the file to something comprehensible and saves the data in to a matlab file. Then offpress.m, plots the data near the surface and makes the user select a pressure offset to apply. The aim of this is to have pressure zero at the start of the pressure record. This function removes the data where the *pumps* variable is 0 (meaning the pump of the CTD was off). Spike_t90.m check the dataframe and sets to NaN the large single point spikes in the variables. This routine also calculates salinity by calling several seawater routines. The routine wake.m removes the data when the same pressure level is sampled twice and attempts to find a point where it has the same temperature as in the beginning of the wake and accepts the data from that point. The routine Interpol.m finds any data set to NaN on the variables and interpolates them to get a continuous dataset. The function splitcast.m splits the data in to an upcast and a downcast file. And finally, the ctd2db.m routine does a 2 dbar binning of the CTD downcast data produced before to obtain the final file.

Potential density, absolute salinity, and conservative temperature are not calculated in the CTD processing. To calculate them, I used routines from the GSW oceanographic toolbox Version 3.03 (R2011a) (23/05/2013). The thermodynamic equation of seawater (TEOS-10, 2010) was adopted by the Intergovernmental Oceanographic Commission at its 25th Assembly in June 2009 to replace the EOS-80 as the official description of seawater and ice properties.

Under TEOS-10, all the thermodynamic properties of seawater depend of absolute salinity (g/kg) rather than practical salinity (nondimensional), so the calculation of it is one of the first steps in processing oceanographic data (IOC *et al.,* 2010). To calculate it, I used the GSW function "gsw_SA_from_SP" (Jackett *et al.,* 2013; Version 3.04) which calculates the absolute salinity from the practical salinity (given by the CTD). This function interpolates the Global Absolute Salinity Anomaly Ratio (R^{δ}) (in the GSW library) to the pressure, longitude and latitude, and then uses the interpolated value of (R^{δ}) to calculate absolute salinity following this expression: (3)

$$S_A = \frac{35.16504\ g\ kg^{-1}}{35} S_p\left(1 + R^{\delta}\right) \quad (3)$$

where S_A is absolute salinity, $\left(\frac{35.16504\ g\ kg^{-1}}{35} S_p\right)$ is the reference salinity S_R which is the best estimate of absolute salinity of an standard seawater sample, S_P is the practical salinity.

From the potential temperature, I calculated the conservative temperature, with the GSW function "gsw_CT_from_PT.m" (Jackett *et al.*, 2013; Version 3.04). Conservative temperature is proportional to conservative enthalpy. Conservative temperature depends on absolute salinity, potential temperature and pressure.

Potential density was calculated by using the function "sw_pden" (Morgan and Pender, 1992; modified by Pender, 2012). In this study I use the potential density anomaly which follows the equation (4):

$$\sigma_\theta = \rho_\theta - 1000\ kg\ m^{-3} \quad (4)$$

Where ρ_θ is the potential density at a reference pressure (ocean surface).

To assess stratification, I calculated the squared buoyancy frequency (Brunt-Väisälä-frequency) N^2 with the GSW function "gsw_Nsquared.m" (McDougall and Barker, 2016; Version 3.05.6). The Brunt-Väisälä frequency is a measure of the vertical stability of a fluid, and it can be used to assess stratification.

$$N^2 = g^2 \rho \frac{\left(\beta^\theta \Delta S_A - \alpha^\theta \Delta\theta\right)}{\Delta P} \quad (5)$$

where ΔS_A and $\Delta\theta$ are the differences between absolute salinity and conservative temperature in adjacent water parcels separated in the water column by the gradient in pressure of ΔP. β and α are the saline concentration and thermal expansion coefficient evaluated at the averages of absolute salinity, conservative temperature and pressure, g is the gravitational acceleration.

The mixed layer depth (MLD) was calculated in two steps. First, I checked graphically the density profile and the density gradient profile of each station. The density gradient was calculated following formula (6):

$$Density\ Gradient = (\rho_{z_2} - \rho_{z_1})/(z_2 - z_1) \quad (6)$$

Once the density gradient (6) and the density profile was plotted, I checked visually at which depth the pycnocline started for each station in every year. Based on that, I determined a density gradient threshold of 0.01 kg m^{-4} as the upper limit of the pycnocline. I defined the MLD as the depth at which the density gradient defined before was above 0.01 kg m^{-3} for the first time in the water column. Due to the presence of deeper mixed layers in many years, I defined two mixed layers based on the same criteria, having a water column distributed as: Mixed layer, first pycnocline, second mixed layer and pycnocline.

3.3 Water Sampling:

Water samples for analyses of the nutrient and chlorophyll *a* (Chl *a*) concentration were taken with Niskin bottles mounted on the CTD frame at 6 different depths (0, 5, 10, 20, 50 m, and bottom) during the upcast. The sub-samples for the nutrient concentration were taken first and stored in a 50 mL Falcon tube in a freezer at -20 ºC. Then, 2 L of seawater were taken from the bottles for analyses of the Chl a concentration and stored in drums in the cooling room (3 ºC-4 ºC and darkness) until filtration.

3.4 Nutrient data analysis:

Nutrient data was analysed at UiT by standard seawater methods by using a Flow Solution IV analyser from O.I, Analytical USA. The analyser was calibrated with reference seawater from Ocean Scientific International ltd. UK.

3.5 Chlorophyll a filtration and analysis:

Triplicates of 200 mL were filtered for each sampling depth (0, 5, 10, 20, and 50 m). The filtration process was conducted twice to get the size fractionated chlorophyll *a* concentration. A Whatman GFF filter was used to get determine the total Chl *a* concentration (> 0.7 µm).

The carboys with the samples were gently mixed six times to the cell sedimentation while stored in the cooling room. After that, samples were filtered at a pressure of 5 dbar. Once the samples were filtered, the filters were stored in aluminium foil in the freezer (-20 ºC) for later analysis at UiT. The analysis at UiT was conducted within five months. The filters were defrosted and extracted for 24 h in 96 % ethanol. Then the Chl a concentration was measured in a Fluorometer (Turner Designs) following the acidification method by Holm-Hanssen & Riemann (1978).

3.6 Meteorological data

Meteorological data were downloaded from the Norwegian Meteorological Institute at eklima.no. Wind data in form of wind speed and direction were obtained from Skrova in Vestfjorden (figure 2). The data obtained had a resolution of one measurement each 6 h, which were averaged per day to facilitate the reading of the plot.

To transform the wind direction and the intensity of the wind speed, vector speed was converted to the two eastward and northward components of the wind vector speed (u and v) so the data can be plotted according to:

$$u = \left|v_{speed}\right| \sin\left(\frac{\pi}{180} \cdot \theta\right) \tag{7a}$$

$$v = \left|v_{speed}\right| \cos\left(\frac{\pi}{180} \cdot \theta\right) \tag{7b}$$

where u is the eastward X component of the wind speed vector, v is the northward Y component of the windspeed, $\left|v_{speed}\right|$ the intensity of the wind speed, and θ the wind direction in degrees.

Temperature data was not available at Skrova and therefore obtained from the meteorological station in Bodø.

River runoff data represent the freshwater input to Vestfjorden from the rivers in the mainland and is given in $m^3\,d^{-1}$.

4 Results

4.1 Meteorology and freshwater runoff

Air temperature varied a lot between March and April of every year (figure 4). Temperature in April was more uniform (from 2014-2019). Maximum and minimum temperature were recorded in 2019 (-8.3 and 14.1 ºC; Table II). The difference between maximum and minimum temperature varied a lot interanually from 2014-2018, and in 2019 almost doubled compared to the previous years.

Wind data showed a large variability between the years. Predominant wind direction in 2014 and 2015 was from south west (SW). In the week prior to the cruise in 2014, very strong S/SW winds (stronger than 12 m/s) were observed at Skrova, whereas in 2015 there was a mix between SW winds and westerly winds (W). In the week prior to the cruise in 2016, there were strong SW winds (> 10 m/s) which changed to weaker NE winds (~6-9 m/s) after the first CTD transect was taken (02/04/2016; figure 3). After the second CTD transect was taken (07/04/2016; figure 3), the wind changed to relatively calm conditions with low wind speed and variable direction. The cruise in 2017 did not show any clear pattern in terms of wind in March in April with shifting wind directions. In 2018, there were relatively calm conditions the week before the cruise with weak westerly winds (W). The year 2019 was characterized by strong S winds which change to similarly strong SW wind the week before the cruise.

Table II Air temperature in Bodø from March and April 2014-2019. The range in the temperature average is the standard deviation. The maximum and minimum temperatures are for the entire March-April period.

Year	Average air temperature (ºC) March	Average air temperature (ºC) April	Maximum Air Temperature (ºC)	Minimum Air Temperature (ºC)	T difference (ºC)
2014	2.0 ± 3.5	3.9 ± 1.7	6.4	-6.5	12.9
2015	2.9 ± 2.3	4.0 ± 1.2	6.9	-1.1	8
2016	2.4 ± 2.9	4.3 ± 2.0	9.7	-3.6	13.3
2017	0.6 ± 2.7	2.1 ± 1.8	5.8	-4.8	10.6
2018	-2.6 ± 2.8	3.7 ± 2.8	7.5	-6.8	14.3
2019	-0.8 ± 5.5	5.5 ± 4.5	14.1	-8.3	22.4

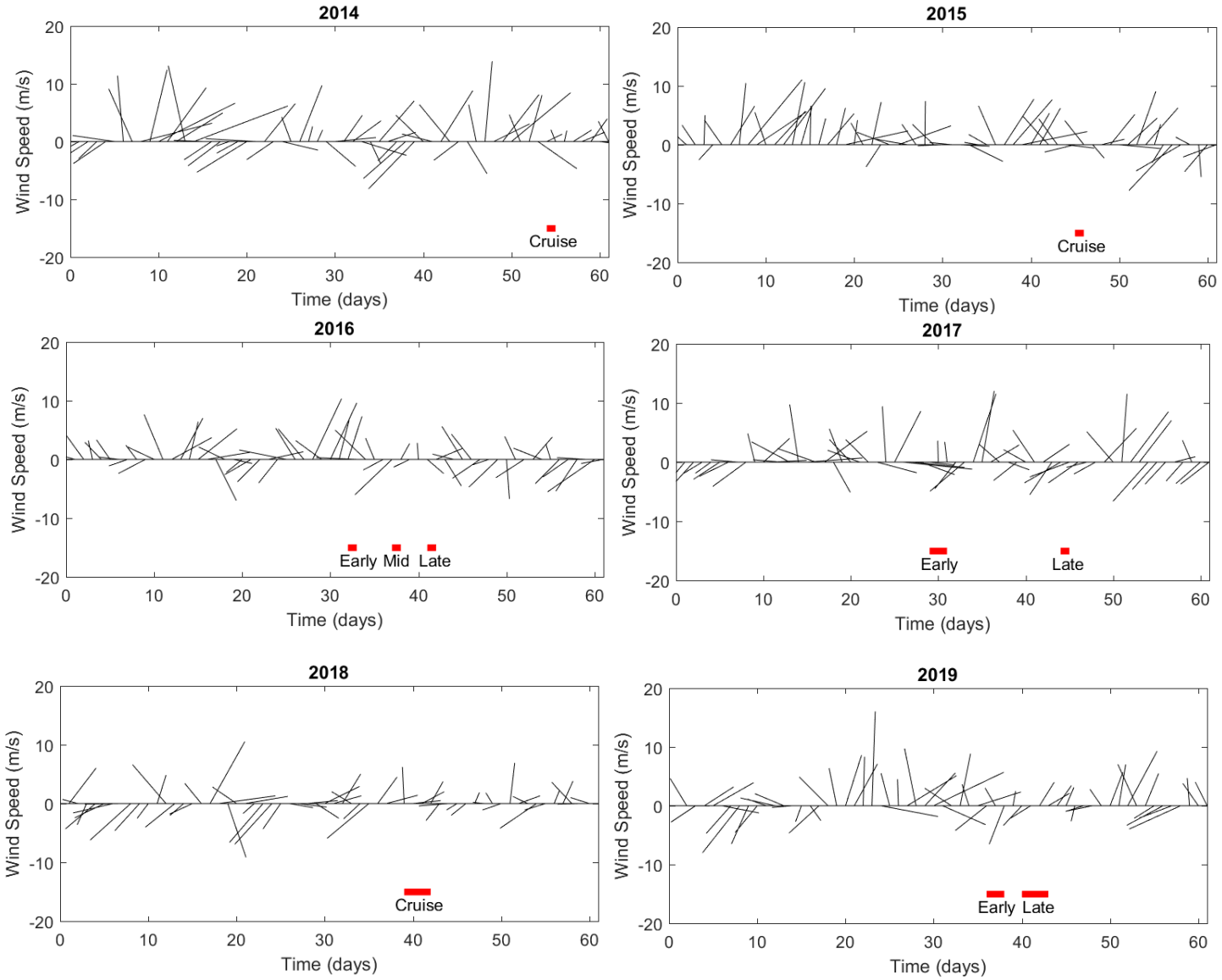

Figure 3 Wind vectors from 01/03 (day 0) to 30/04 (day 61). The length of the vector indicates the strength of the wind, and the direction of the vector the direction of where the wind is blowing to. The red lines on the bottom show when the CTD transects (figure 2) were taken.

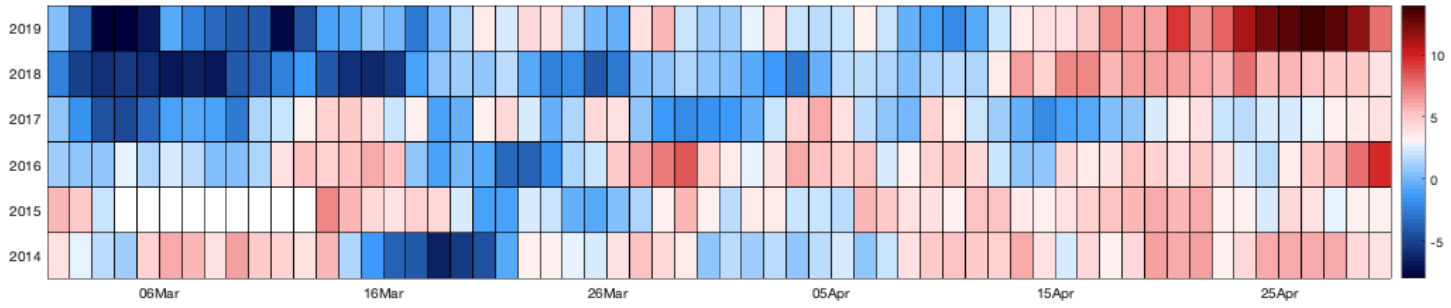

Figure 4 Hovmöller diagram of the air temperature (ºC) of each year. Each cell represents a day.

Daily freshwater input to Vestfjorden from rivers on the Norwegian mainland in spring is characterised by large day-to-day variability with short-term events of high discharge (figure 5). In 2018, the daily average runoff is very low (~ 200 m^3 s^{-1}) until the end of April. The freshwater runoff in 2019 presented periods of high discharge (> 1100 m^3 s^{-1}), and periods of very low discharge (~ 200 m^3 s^1). Cumulative freshwater input to Vestfjorden due to river runoff increases near linearly in March and April in all years (figure 5). The year 2018 presented the lowest values of cumulative freshwater input into the fjord (~ 1.2 km^3) whereas 2019 presented the highest cumulative discharge (~ 3.1 km^3). The other years ranged between 1.7 to 2.5 km^3.

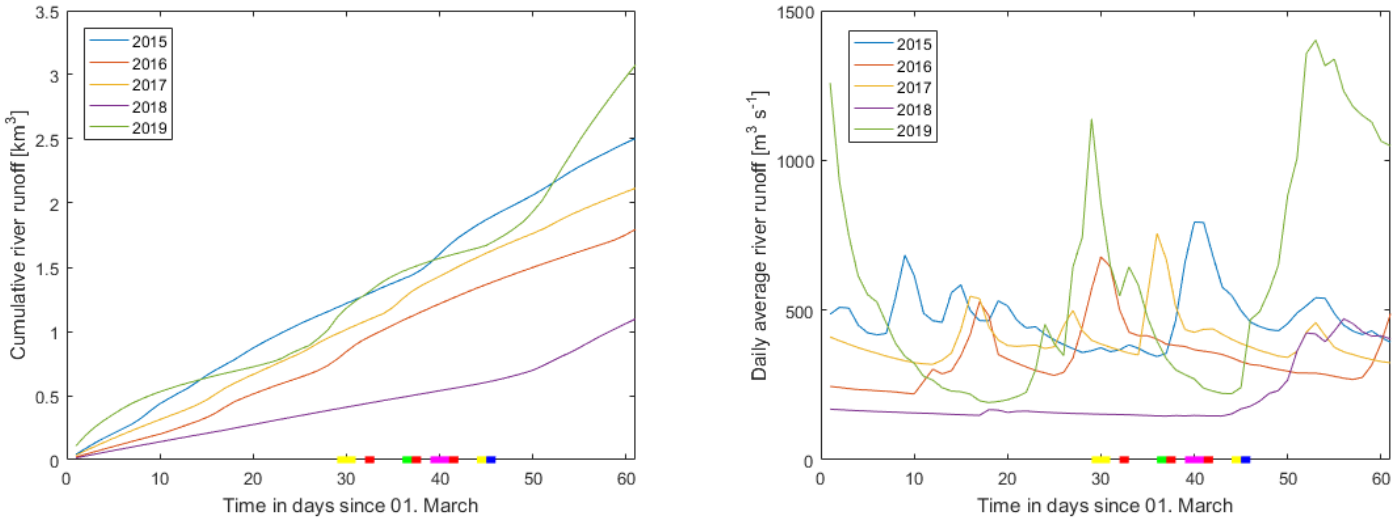

Figure 5 Cumulative river runoff (km^3 in Vestfjorden (on the left). On the right daily average runoff (m^3 s^{-1}). On the X axis the colours represent the different cruises. Blue for 2015, red for 2016 April I, II and III, yellow for 2017 March and April, purple for 2018 and green 2019.

4.2 Hydrography

4.2.1 Temperature

The water temperature in Vestfjorden was comparable to a typical high latitude spring temperature profile (Cottier *et al.*, 2010) with colder (3 - 4 ºC) water above the thermocline layer and higher temperatures (7 – 7.5 ºC) below the thermocline. Below 100-200 m, the temperature was constant at around 7.5 ºC (figure 6). There was a horizontal gradient in the surface layer with colder waters from the inner part of the fjord (~68.4 ºN) to warmer waters in the outer part of the fjord (~67.9 ºN) (Table III).

Table IIIII Horizontal temperature difference (2014-2019) from inner (station 1) fjord to outer fjord (station 6).

Cruise	2014	2015	2016 I	2016 II	2017m	2017a	2018	2019
T difference (ºC)	0.604	0.6317	0.9725	0.3829	0.3159	0.2938	0.5148	0.3087

The vertical temperature gradient was smaller in 2014 and 2015 than in the other years (2016, 2017, 2018, 2019). For example, in 2014 one of the smallest vertical gradients was found, with temperatures in the surface of 4.3 – 5 ºC and > 6.8 ºC below 150 m. On the other hand, in 2018 the largest vertical temperature gradient across the whole section was found. Temperature increased from 2.8 – 3.2 ºC the at surface to > 7 ºC below 120 m. The inner stations (station 1, 2, 3) showed stronger temperature gradients than the outer stations, with a colder surface temperature (< 3 ºC). The decrease on depth around 68.1 ºN affected the water column. This can be observed by the presence of either an eddy (2016, possibly 2018, 2019) or a front (2014, 2016, 2017). In 2018, the temperature in the surface layer was much lower than in the other years, especially at the central stations (< 3 ºC) (station 3b and 4) (figure 6).

Short term changes in water temperature could be observed in the years 2016 and 2017. In 2016 and 2017, the transect was sampled three and two times, respectively, within April, which allowed to investigate the changes in the hydrography during the period of the phytoplankton spring bloom. In *April I 2016* (01 April to 02 April), the vertical displacement of the isothermals showed the presence of a strong front between inner and outer fjord at around 68.1 ºN. By April II, the front could not be observed, probably because it was pushed outwards of the fjord (southward towards the mouth of the fjord) or disappeared (06 April to 07 April) (*April II 2016)*. By the end of the cruise (*April III 2016*) (10 April), the bumping of the isothermals showed the presence of a warm core cyclonic eddy back at 68.1 ºN.

In March 2017 (29 March), the all the stations except station 6, were strongly temperature stratified, with temperature ranging from 3.3 – 3.8 ºC in the surface and reaching the 7.4 ºC shallower (~80 m) than in the other years. The outermost part was less stratified; the 7.4 ºC isothermal was deeper (100 m) than at the other stations, and the surface temperature was higher hence, a smaller vertical temperature gradient was found. In April 2017 (23 April to 24 April), the vertical temperature gradient in the outer stations (station 5 and 6) got smaller compared with the inner stations (station 1, 2, 3). This is shown as the surface temperature is higher than the inner fjord (~ 4.5 – 5 ºC) and the 7.4 ºC isothermal is deeper than at the inner stations (100 m on stations 5 and 6 and 70m in stations 1, 2, 3 and 4).

4.2.2 Salinity

Similar to temperature, salinity followed a typical high latitude spring salinity profile (Cottier *et al.,* 2010). The surface layer down to 50 m presented a salinity of (33 – 34 g kg^{-1}) whereas from 100 m to the bottom salinity was rather constant (~ 34.9 g/kg; figure 7). In the surface layer, there was a horizontal salinity gradient from the inner to the outer fjord with fresher water in the inner part than in the outer part (figure 7). At 68.1 ºN, where the bottom topography changes, the presence of eddies and fronts was detected.

In the years 2014, 2015, and 2018 a weak vertical salinity gradient was found, with the saltiest surface layer (~ 33.7 g/kg in the inner fjord and 33.7 – 34.1 g/kg in the outer fjord) in 2018. During the other years (2016, 2017, 2019), a fresher surface layer and a stronger halocline was observed. In 2017, the surface layer was freshest (< 32.9 g/kg). From March 2017 (29 March) to April 2017 (23 April to 24 April), a strengthening of the halocline occurred at the inner stations (figure 7) due to a freshening of the surface layer. However, in the outer stations (St 5, 6) there was a slight increase in salinity at the outer most stations (from 33.3 g/kg to 33.5 g/kg), thus decreasing the strength of the halocline there.

In the year 2016, in *April I 2016* (01 April to 02 April), the salinity signal indicated also a front at the location where the temperature front was (figure 7) at 68.1 ºN, which disappeared being pushed outwards (~67.8 ºN) (06 April to 07 April) (*mid 2016)* as well as the temperature front. In the last transect taken (*late 2016*) (10 April), the front disappeared and showed the presence of a cyclonic eddy.

4.2.3 Density:

The general features in density result as a combination of the temperature and salinity distribution, therefore, the main characteristics are still present in the density distribution. In general, inner stations present a stronger pycnocline than outer stations due to the presence of the horizontal gradient in the top layer, but the presence of a bottom water mass with a constant potential density (> 27 kg m^{-3}) below the pycnocline.

Following the temperature and salinity distribution, there was also a horizontal gradient of density on the fjord, with denser water at the outer stations. The heaviest water in the surface (26.7 – 26.9 kg m^{-3}) was observed in 2018. The bottom density in 2018 is similar to the rest of the years (~ 27.1 kg m^{-3}), thus having the smallest density gradient from surface to the bottom in all the years.

Table IIV Mixed layer depth (m) for each station and year. When more than one depth is given, a second ML was detected. In that case, the first value indicates the depth of the shallow ML and the start of the first pycnocline. The depth range after represents the start of the second ML, and the start of the second pycnocline. When < 10 m is shown, the ML was shallower than 10 m. Mixed is used when the water column is mixed

Transect	**st1**	**st2**	**st3**	**st4**	**st5**	**st6**
2014	15	x	86	29	16 // 17-54	16 // 22-61
2015	13 // 22-69	13-28 // 30-60	13-18 // 19-87	31 //32-82	?	35 // 41-94
2016 AI	22 // 28-49	20 // 23-51	35 // 37-49	39 // 44-64	29	66
2016 AII	< 10	19	31	25	35	mixed
2016 AIII	x	x	x	x	x	x
2017m	50	28 // 30-62	28 // 29-48	40	25 // 26-42	32 // 33-50
2017a	12 // 21-30	33	34	15 (32)*	32	30
2018	46	29	38	54	49	38
2019	20-57	31 // 34-60	53	22 // 26-43	63	27

The Rossby radious of deformation in the deeper areas of the fjord is 5.7 km whereas in the shallower areas (i.e., station 6), of 2.8 km. Therefore, the effects of rotation will have importance in Vestfjorden.

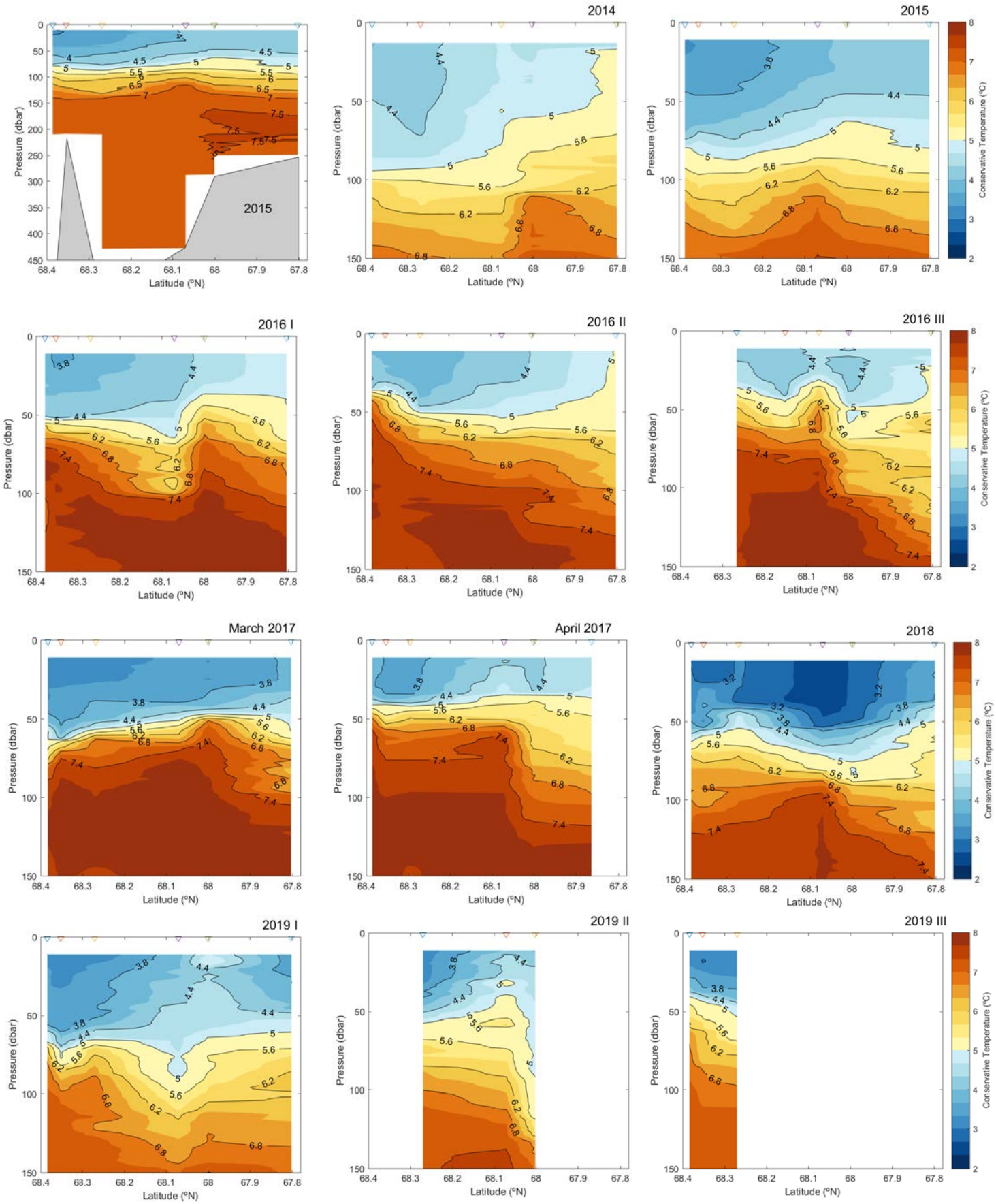

Figure 6 Conservative temperature (ºC) distribution of the central transect in Vestfjord (figure 2) in the different cruises. The first plot gives an overview of the full depth temperature (ºC) distribution and the rest is limited just to the 150 m first meters in the water column. The stations are noted in the superior X axis with coloured triangles. Isolines represent temperature (isothermals). The interval between isothermals is 0.6 ºC.

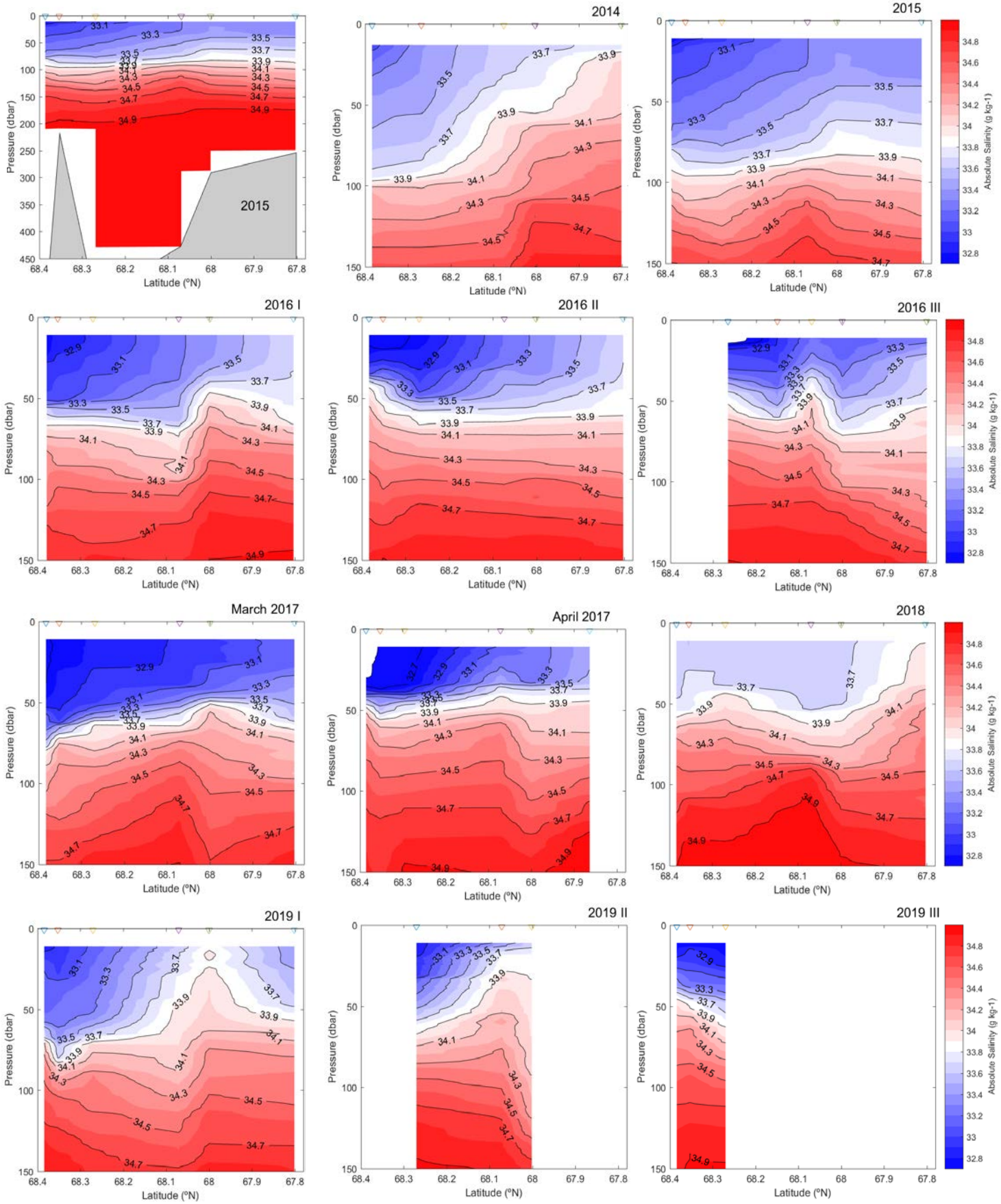

Figure 7 Absolute salinity (g kg^{-3}) distribution of the central transect in Vestfjord (figure 2) in the different cruises. The first plot gives an overview of the full depth salinity (g kg^{-3}) distribution and the rest is limited just to the 150 m first meters in the water column. The stations are noted in the superior X axis with coloured triangles. Isolines represent salinity (isohalines). The interval between isohalines is 0.2 g kg^{-3}

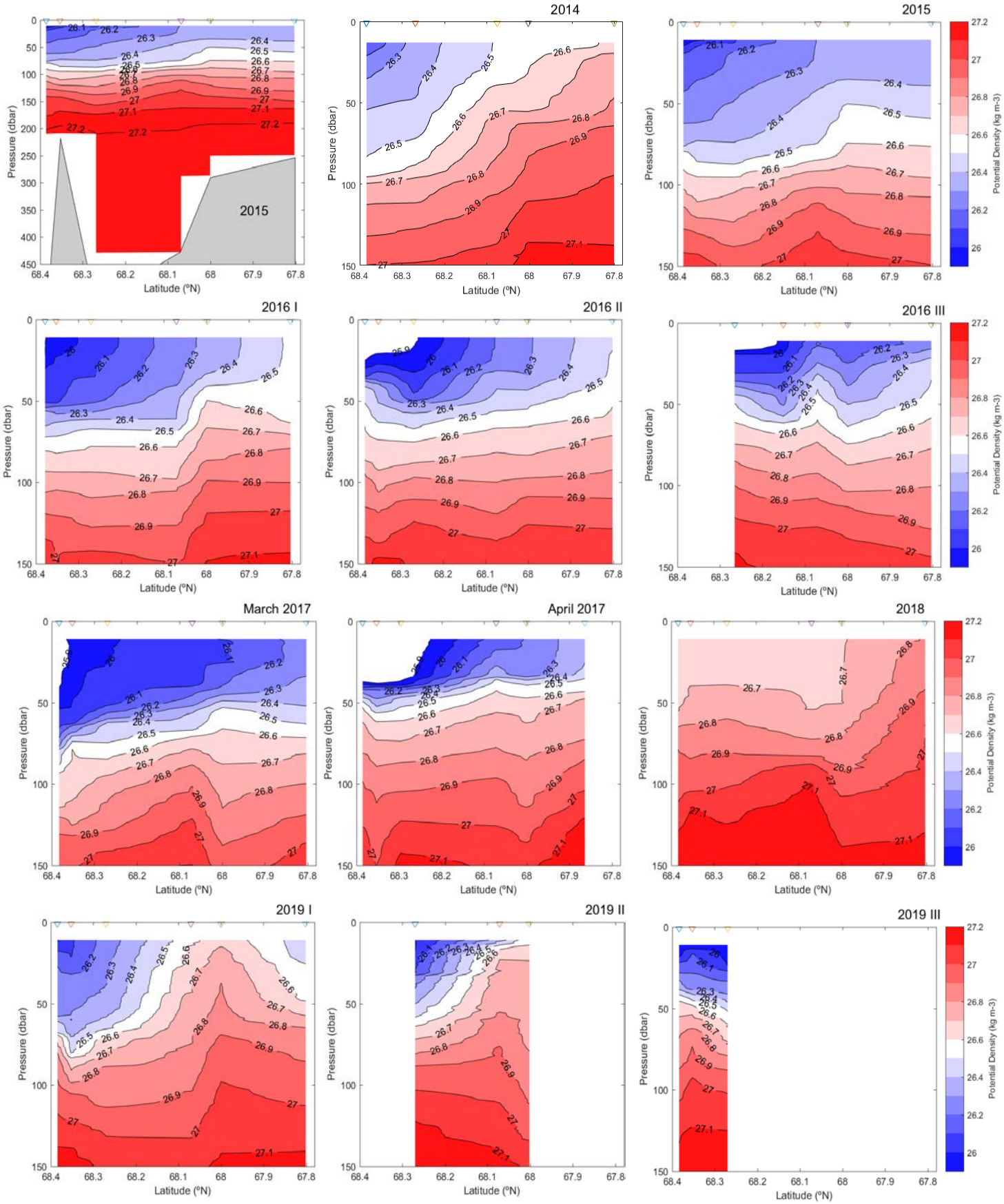

Figure 8 Density distribution of the central transect in Vestfjord (figure 2) in the different cruises. The first plot gives an overview of the full depth density distribution and the rest is limited just to the 150 m first meters in the water column. The stations are noted in the superior X axis with coloured triangles. Isolines represent density (isopycnals). The interval between isopycnals is 0.1 kg m^{-3}

4.3 Biological parameters

4.3.1 Fluorescence and chlorophyll a (Chl a)

Fluorescence, a proxy of the autotrophic biomass in the water column, varied between the years. As the autotrophic biomass depends on light, the fluorescence was always higher at the surface, and near zero below 50 m.

In 2014, fluorescence intensity was low along the transect in Vestfjorden (1.5 – 2.5). Maximum values are observed in the upper water column (20 m) and the signal of the fluorescence is not zero above the 26.8 kg m^{-3} isopycnal in the whole transect (figure 9) at around 110 m in the inner stations and 75 m in the outer stations being much deeper that the other years.

In 2015, a higher fluorescence intensity (figure 9) was found than during cruises of the other years, even though the water column was less stratified. In the outer stations, the bloom was at its maximum with values over 4 until 45 m depth, following the 26.4 kg m^{-3} isopycnal. In the inner fjord values of fluorescence were slightly smaller ranging between 2 and 3.5 until the same depth fjord, but independently to the density (the maximum density at which the fluorescence signal is not null is not constant).

In 2016 fluorescence intensity (figure 9) showed a differentiation between the inner fjord and the outer fjord. The inner fjord, (st 1, st 2, st 3b) presented low values (0.5 – 1.5) at the three different periods (Early, Mid, Late). However, the outer fjord had the bloom ongoing in the three periods, with values ranging from (2 – 4) being very linked to the density distribution (see discussion). The bloom was located at surface in the first two periods, *early 2016* (01 April to 02 April) and (*mid 2016*) (06 April to 07 April) whereas in the last period, (*late 2016*) (10 April), the bloom, especially in the outer most stations was located in a subsurface chlorophyll maximum at around 20 – 25 m.

In 2017, both march (29 March) and April (23 April to 24 April), presented very low values (< 2). Values ranged from 1 – 2 above the pycnocline and in the whole transect (with higher values in the outer fjord) in March, whereas in April, the higher values were close to 1 in the outer station.

In 2018, higher values are in the inner fjord and the middle, with a will-mixed water column until down to 50 m. Fluorescence was not uniform with depth, with the highest concentration associated to a density front in the middle fjord (st 4) (see discussion).

In 2019, fluorescence is highly associated to density distribution (eddy in the outer fjord and front in the inner fjord) (see discussion) and therefore values are very variable along the transect.

4.3.2 Nutrient concentration

NO_3 + NO_2

During all the years, the lowest nitrate concentration was found in the uppermost 20 m of the water column, while below 50 m the nitrate concentration was always high (> 9 mmol nitrate m^-3). I decided here to pool the years into two groups: the years in which the surface layer was nutrient low (< 2 mmol nitrate + nitrite m^{-3}), and in years where the nitrate concentration was not limiting (> 2 mmol nitrate + nitrite $m^{-3)}$. The years that presented depletion in the first 20 m were 2015 and 2018. And the rest, 2016 early and late and 2017 had values above 2 mmol m^{-3} of nitrate. The year with strongest depletion in the surface layer was 2015, with values below 0.3 mmol m^{-3} in the outer stations (st 4, 5, 6) and values between 1 – 1.6 mmol m^{-3} in the inner stations (st 1, 2, 3). In the cruises with a nitrate + nitrite depleted surface, there was the presence of a horizontal nutrient gradient in the first 20 m of the water column. This gradient was stronger in 2015, with nitrate concentrations being 4 times bigger in the inner fjord (1.3 – 1.6 mmol m^{-3}) than in the outer fjord (below 0.3 mmol m^{-3}). In 2018, the concentrations were double inner stations (~ 2 mmol m^{-3}) than in the stations outer stations (~ 1 mmol m^{-3}).

During the early transect of 2016 and March 2017, surface was nutrient rich, especially in 2017 with concentrations above 20 m between 2 and 3.3 mmol m^{-3} in all the transect. In 2016, station 6 presented an extremely high nutrient concentration with values between 5 – 6 mmol m^{-3}. In the years without a nutrient depleted surface, there is a concentration minimum varying between 5 – 20 m..

$SiOH_4$

As well as with nitrate, surface (first 20 m) silicate concentrations were the lowest in all the years. As for nitrate and nitrite concentration, the years that presented nutrient depletion were 2015, 2016 early, 2016 late and 2018. The year with lowest surface silicate concentration was 2015 and 2016, with similar concentrations ranging from 0.3 to 1.6 mmol m^{-3}. The most nutrient depleted stations in both years are station 4 and 5 (< 0.6 mmol m^{-3}).

The surface layer in 2017 is the only one that does not present a surface with nutrient depletion. The silicate concentration did not constantly increase with depth (as nitrate + nitrite did) but was high at surface. (Although, and same as for the nitrate concentration, there are subsurface concentration minimum between 5 – 20 m, with a huge difference from the highest value in that station. E.g: station 5 at 0 and 5 m presents values of around 3 mmol m^{-3}, whereas at 10 m, the concentration reduces down to approximately 0.5 mmol m^{-3}.

PO_4

Phosphate nutrient concentrations are much lower if comparing them with the silicate and nitrate. All the years present very low concentrations (below 0.5 mmol m^{-3}) down to 50 m. Concentrations are rather constant in depth and horizontally.

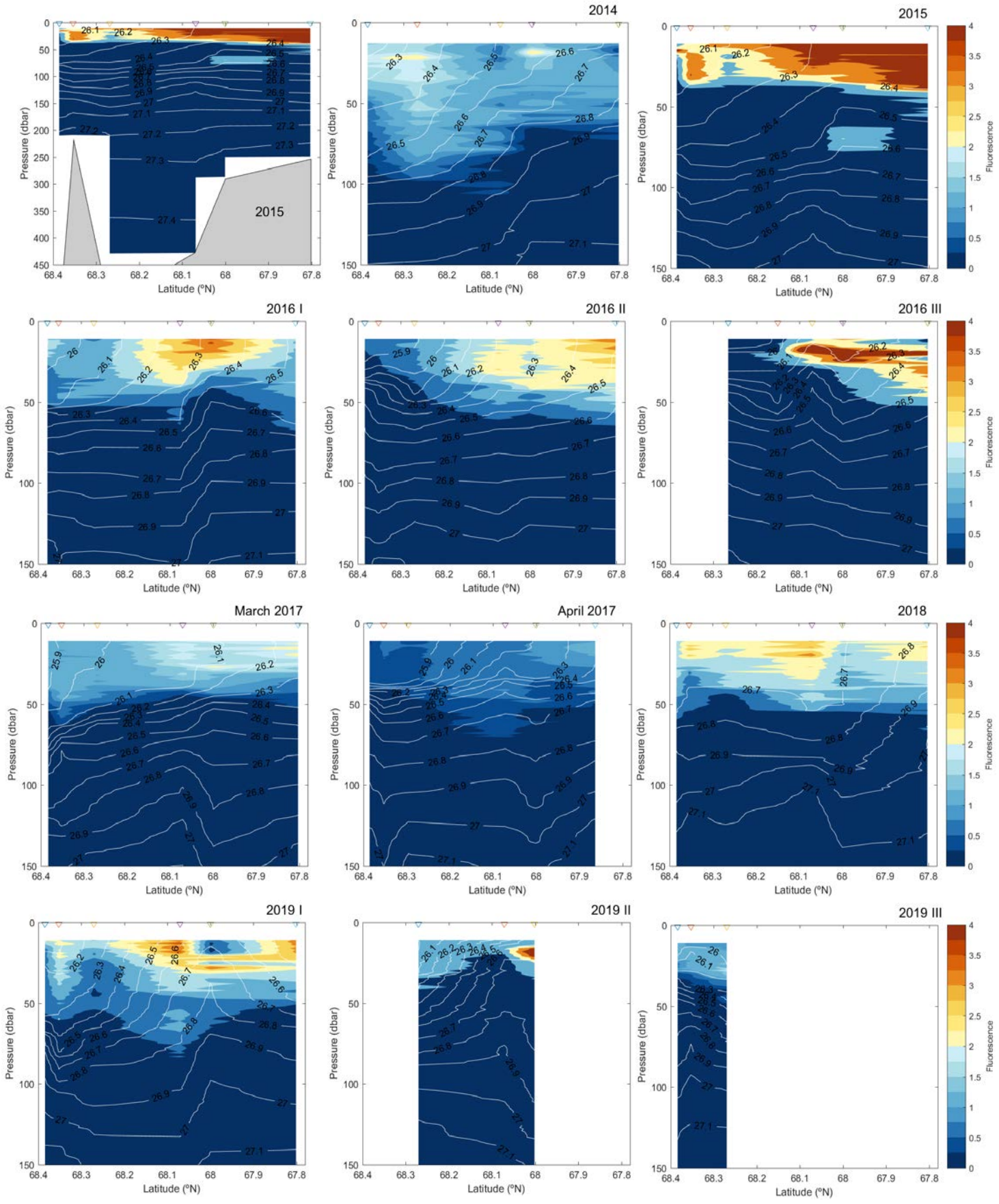

Figure 9 Fluorescence intensity distribution of the central transect in Vestfjord (figure 2) in the different cruises. The first plot gives an overview of the full depth fluorescence intensity distribution and the rest is limited just to the 150 m first meters in the water column. The stations are noted in the superior X axis with coloured triangles. Isolines represent density (isopycnals). The interval between isopycnals is 0.1 kg m^{-3}.

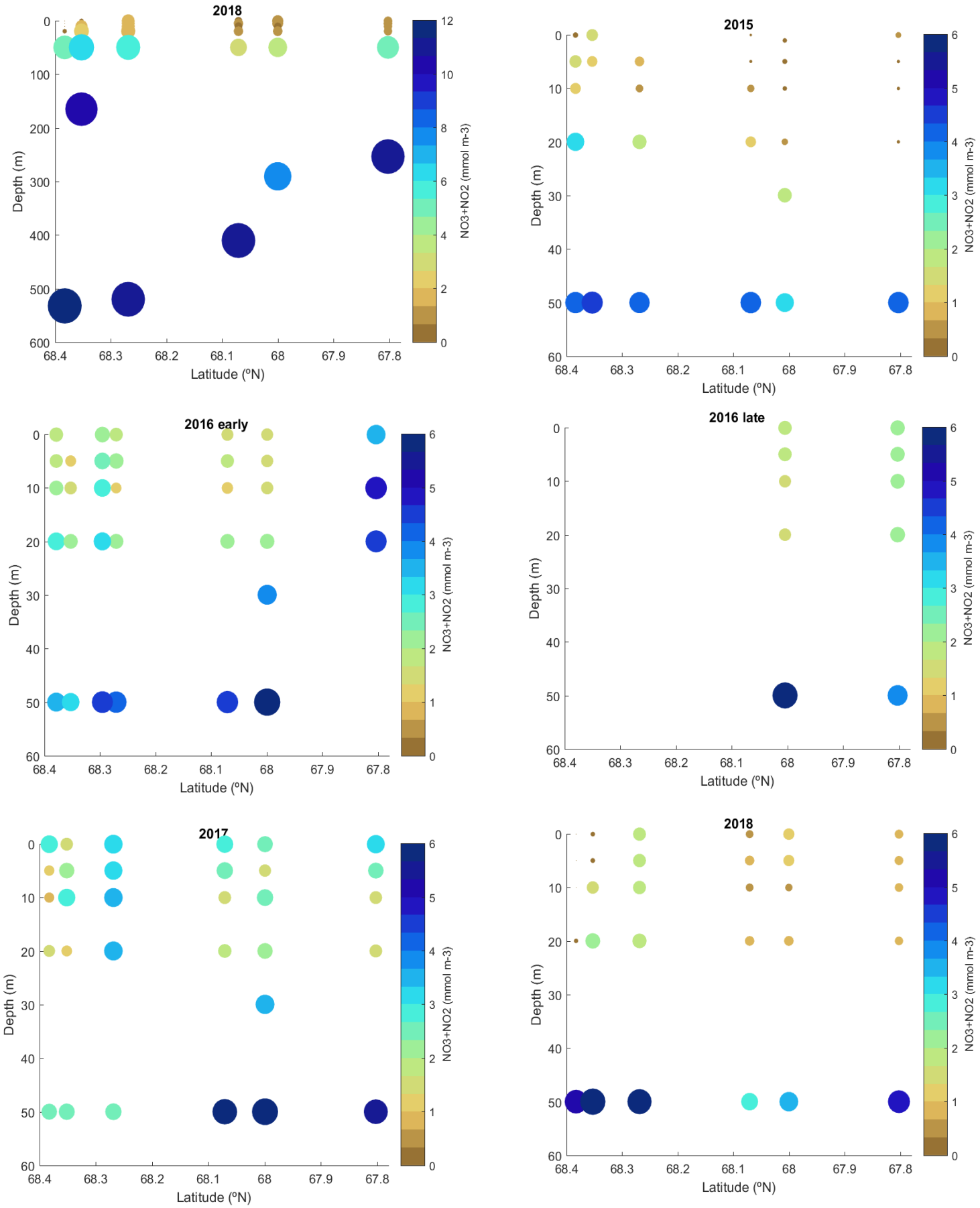

Figure 10 $NO_3 + NO_2$ concentration along the transect in Vestfjorden. Colour represents concentration as well as the size. Bigger circles represent bigger concentrations. Each point is where a water sample was taken. The missing points mean that there was a missing sample.

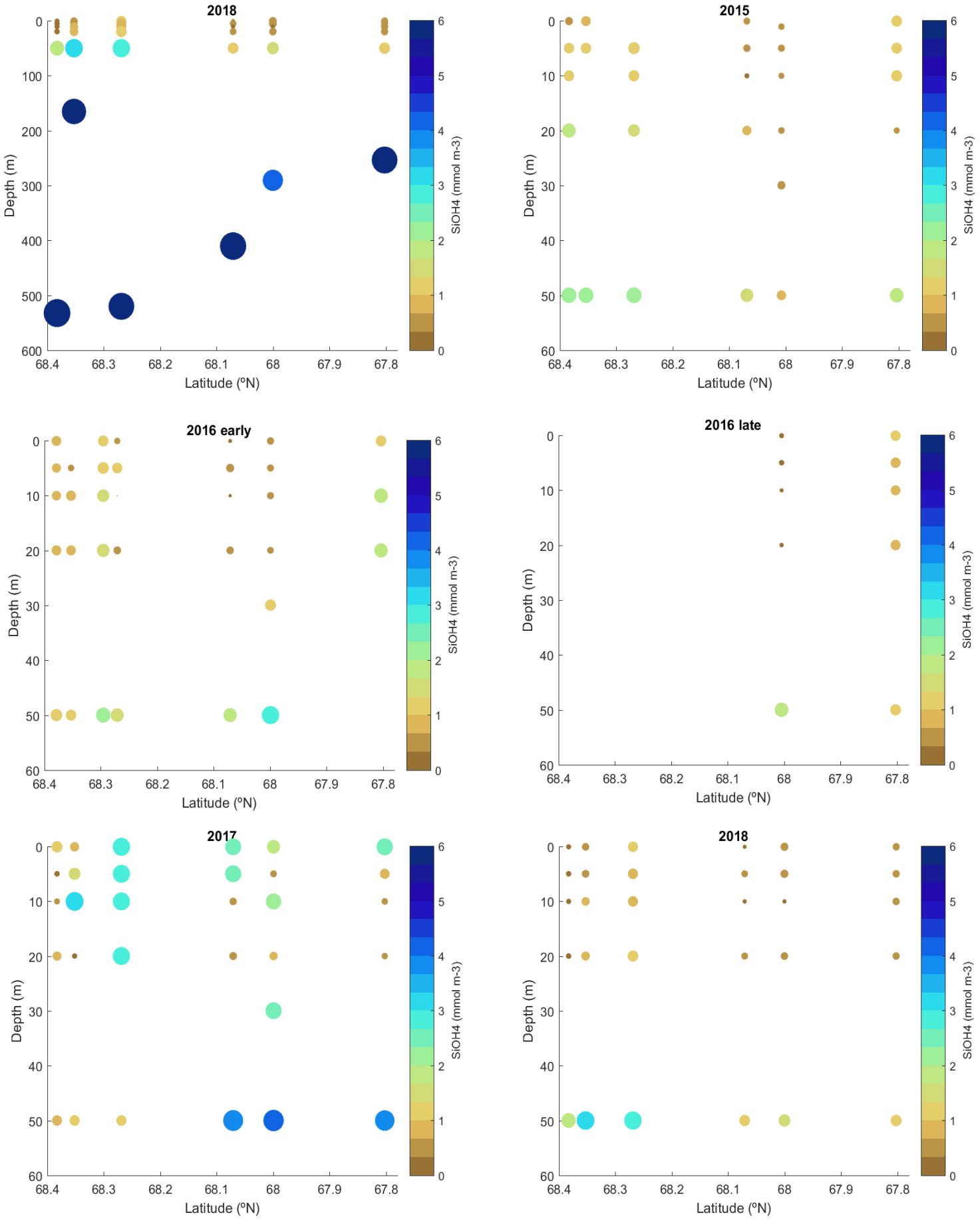

Figure 11 $SiOH_4$ concentration along the transect in Vestfjorden. Colour represents concentration as well as the size. Bigger circles represent bigger concentrations. Each point is where a water sample was taken. The missing points mean that there was a missing sample.

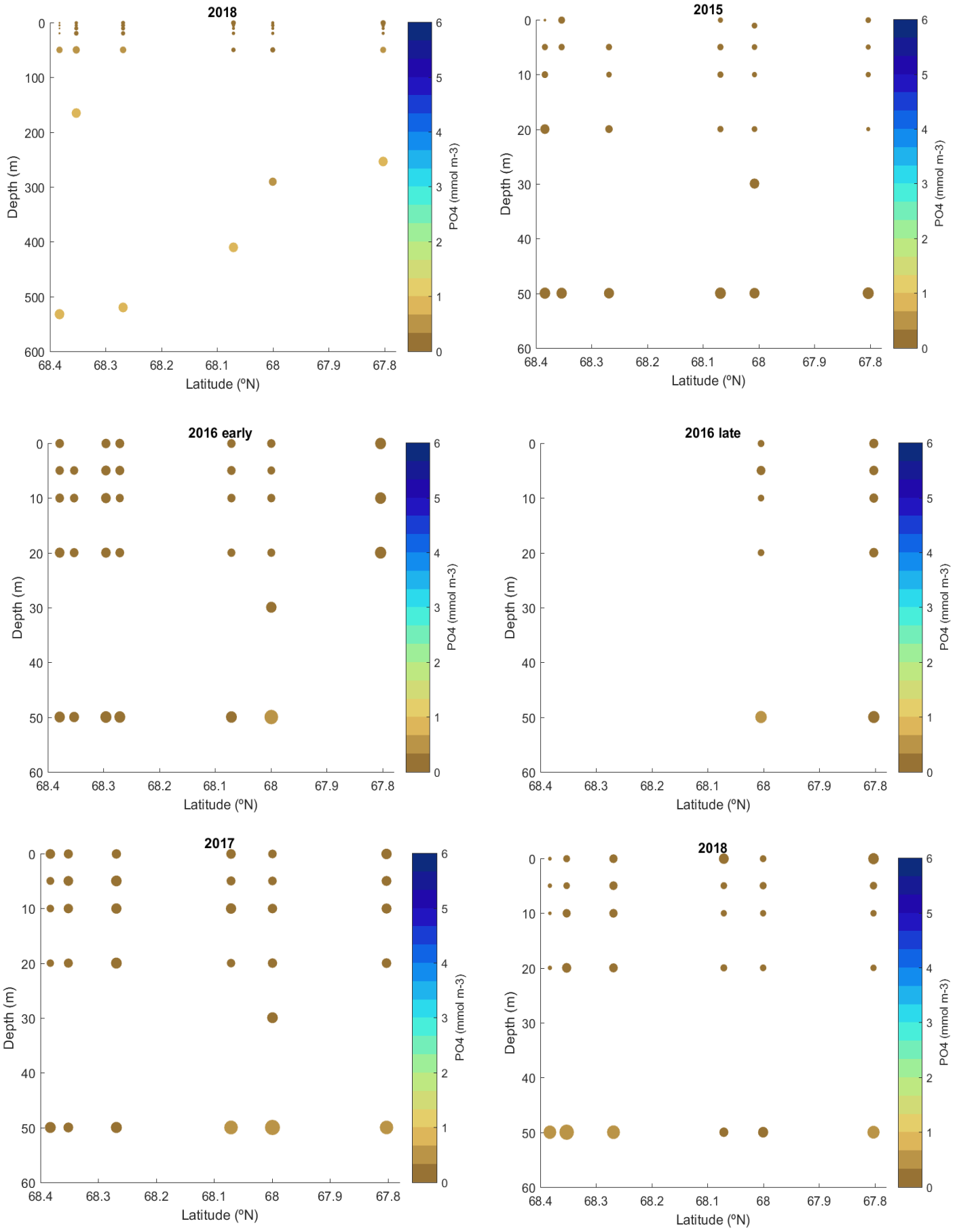

Figure 12 PO_4 concentration along the transect in Vestfjord. Colour represents concentration as well as the size. Bigger circles represent bigger concentrations. Each point is where a water sample was taken. The missing points mean that there was a missing sample. NOTE: In this figure the size scale has been multiplied times 4 to be allowed to see the changes in concentration. The color scale remains the same compared with the other nutrient figures, so if wanting to compare this figure with the other nutrient figures use the colour not the size.

5 Discussion

5.1 Hydrography

5.1.1 Common hydrographic patterns in Vestfjorden

In the study period (2014-2019), Vestfjorden experienced high interannual variability in terms of hydrographical conditions. The surface water temperature and salinity observed in this study match with previous findings for April (Furnes and Sundby, 1981: 2 – 4 ºC / 33 – 34 g kg^{-1}). The bottom layer in this study was warmer (7 ºC – 7.5 ºC) than 40 years ago (6.5 – 7.0 ºC, Furnes and Sundby, 1981). In the 20th century, fjords on Svalbard have been warming (Pavlov *et al.,* 2013), and this is a general process in the world oceans. This process affects also to the NAC (Mork *et al.,* 2019) and the coastal waters (Albretsen *et al.,* 2012). Thus, the differences in bottom temperature in Vestfjorden between earlier observations and the present study could be explained by this general warming. Temperature in the surface of Vestfjorden was in the same range as in Malangen (Wassmann *et al.,* 1996) and higher than the temperatures in Balsfjorden (Eilertsen *et al.,* 1981), Porsangerfjorden and Altafjorden (Eilertsen and Skarðhamar, 2006) in all the years of the study (2014-2019). In Vestfjorden, temperature varies from 3 – 4.5 ºC in the surface during spring same as in Malangen (3.5 – 4.5 ºC). For the same period, the temperatures in Balsfjord ranged from 1.5 – 3 ºC, from 2.2 – 2.6 ºC in Altafjorden and from 2 – 2.3 ºC in Porsangerfjorden. Despite this difference in the temperature, the surface salinity in Vestfjorden and Balsfjorden (no data from Altafjorden and Porsangerfjorden) was rather similar. It ranged in Balsfjord from 32.83 – 33.36 g kg^{-1} (Eilertsen *et al.,* 1981) and in Vestfjorden from 32.6 – 33.9 g kg^{-1}. The biggest difference between the two fjords was the bottom temperature and salinity. In Vestfjorden below 150 m, temperature was rather constant between 7 ºC – 7.5 ºC during the present study, while salinity was observed to be ~ 34.9 g kg^{-1} (figure 6, 7). In Balsfjord, in April, the water column was still fully mixed having then temperatures of ~ 3 ºC and salinities of 33.83 – 33.90 g kg^{-1} (Eilertsen *et al.,* 1981).

The differences in surface temperatures might be caused by different reasons. Balsfjord has different geomorphological characteristics than Vestfjorden, having probably effects on its circulation and water mass distribution. Balsfjord is narrower than Vestfjorden and most importantly it has shallow sills in the entrance (8, 9, and 30 m) (Eilertsen *et al.,* 1981; Eilertsen *et al.,* 1984) thus limiting the exchange on water in and out the fjord. Furthermore, Balsfjorden is much further inland that Vestfjorden therefore experiencing a more land-influenced climate and not getting as much input of coastal waters as Vestfjorden. Therefore, the differences with

Balsfjord are probably caused by, the different physical environment between the two fjords, the position far from the oceanic domain and the warming up of world oceans. Altafjorden and Porsangerfjorden are more Vestfjorden-alike fjords since they are wider and have deep sills. Although, these fjords are located further north than Vestfjorden, explaining why they are colder. Vestfjorden is defined as a coastal bay surrounded by fjords (Mitchelson and Sundby, 2001), therefore it is fair to compare it with a shelf region. Surface temperatures on the shelf of Northern Norway in March ranged from 4.5 – 6 ºC and salinities from 34.3 – 35.1 g kg^{-1} depending of the position of the shelf (Nordby *et al.,* 1999). This is higher than the temperatures in observed during the cruises. The comparisons between Vestfjorden and different northern fjords and the northern Norwegian shelf, allows to affirm that Vestfjorden is in a transition between a shelf area and a true fjord.

There are two main water masses present in Vestfjorden; AW, in the warm a saltier bottom and Coastal Water, in the surface. The Coastal Water is likely to be mixed with the freshwater runoff from rivers in Vestfjorden getting fresher and colder to the head of the fjord. For notation purposes, even if I do not identify it as a new water mass, the mixed coastal water will be call as mNCW from now on.

Both temperature and salinity profiles recorded in Vestfjorden were typical for a high latitude spring (Cottier *et al.,* 2010), with cold and fresh water on top and warmer and saltier water underneath (figure 6, 7). This hydrography pattern had been observed by Furnes and Sundby (1981) in Vestfjorden. The system in Vestfjorden was probably in a transition from a spring to a summer setting (Cottier *et al.,* 2010) during the time of the cruises. The cruises of 2014, 2015, 2016, and April 2017 were the four that happened later in the season. Linked to this, they present the highest surface temperature average and the lowest salinities. The warming and freshening of the surface layer through spring in Vestfjorden, may indicate the transition from a spring profile to a summer profile. In winter, Cottier *et al.,* (2010) assumed a fully mixed ice-covered water column in Arctic high latitude fjords. Due to Atlantic influence, many sub-Arctic Northern Norwegian fjords (not all of them) present boreal temperatures (Wassmann *et al.,* 1996), with Vestfjorden among them (Mitchelson and Sundby, 2001), and therefore are often ice-free year round. This is the case for Vestfjorden, and the deep mixing caused by brine release will thus not happen there. The observations of March 2017 showed a stratified water column. At this time of the year in Balsfjord (Eilertsen *et al.,* 1981), Malangen (Eilertsen and Skarðhamar, 2006) and in the shelf (Nordby *et al.,* 1999) the water column is fully mixed. Therefore, the vertical stratification established earlier in this study than in Balsfjord, starting

in late April/ early May (Eilertsen *et al.*, 1981) and on the northern Norwegian shelf (69º20' N – 70º30'N), where water column stabilisation was delayed until June (Nordby *et al.*, 1999). The stratification in March in Vestfjorden can be due two reasons. Either in winter the water column does not get fully mixed or the stratification onset in Vestfjorden occurs earlier in the year. Although, the constant temperature of the bottom layer suggests that the mixing with the surface layer is not really strong, therefore suggesting that the water column in Vestfjorden does not get fully mixed at any time of the year. During winter, the fjord surface may have typically colder water and saltier water on the surface layer if compared with summer. The cold surface waters are a result of the negative heat fluxes, because the ocean is losing heat to the atmosphere, and this induces convective mixing from the surface downwards. The mixing with the saltier water mass underneath, added to the limited freshwater runoff in winter, makes the surface saltier. Although, the mixing in Vestfjorden seems to be not strong enough to overcome vertical stratification and have a fully mixed water column. The big vertical gradient observed on 2018 (with very cold water on top), supports this idea. Even if the stratification was weaker (less density gradient), the big temperature differences between the surface layer and the bottom layer shows that the water column did not experienced mixing strong enough to mix them up. The reduced freshwater runoff in 2018 (figure 5) and the low air temperatures (figure 4), explain the anomalous surface presented in that year, with the saltiest and coldest waters in the whole study.

During spring, the change to positive heat fluxes induces the warming up in the fjord surface (Cottier *et al.*, 2010). In addition, the increase in air temperature and solar radiation increases the snowmelt on land which, in turn, increases the freshwater runoff, increases stratification, and reduces the salinity of the surface layer. In a typical fjord, the increase of freshwater runoff in spring/summer induce an estuarine circulation (Inall and Gillibrand, 2010). Even if Vestfjorden is not considered as a typical fjord (very wide, deep sill; Mitchelson and Sundby, 2001), the fresher surface water and the horizontal temperature gradient observed in the fjord (getting warmer to the mouth), may indicate the presence of estuarine circulation in Vestfjorden (Inall and Gillibrand, 2010; Cottier *et al.*, 2010). The horizontal gradient is caused by the mixing produced by the shear between the fresh surface outflow of mixed coastal water from the inner fjord and the warmer and saltier (AW) deep inflow in the fjord.

Wind greatly affects the dynamics of a fjord, affecting circulation and mixing of the water masses (Cottier *et al.*, 2010). The topography of the surrounding land of the fjord will steer the direction of the wind (Skogseth *et al.*, 2007; Inall and Gillibrand, 2010; Cottier *et al.*, 2010), a

process that is clearly noted in Vestfjorden (Jones *et al.,* 1997). The dominant SW and NE wind directions (figure 3) indicate the steering of the winds in Vestfjorden. It is assumed that the wind induced mixing (Cottier *et al.,* 2010; Franks, 2014), which, at the time of the surveys of the present study acted over the colder and fresher surface water and mixed them up with the warmer and saltier water below the pycnocline, thus increasing the average temperature and salinity of the surface layer. Freshwater runoff, including precipitation and river runoff, presumably added freshwater to the fjord surface and reduced the average salinity especially in the inner part of Vestfjorden (figure 7). The strong up-fjord (SW) winds prior the cruises of the present study might have increased the mixing of the water column, which also increased the average surface temperature (figure 6) and piled up the water toward the head of the fjord, therefore having more influence from Coastal Water coming from the south. The coastal water coming from the south, is warmer and saltier than a potential mixed Coastal Water (mNCW) from inside Vestfjorden. This, as described by Inall and Gillibrand (2010), might have produced a reversal of the fresh surface outflow, and generated a subsurface current in the opposite direction (outwards). This can be observed in the formation of a downward slope in the pycnocline towards the head of the fjord. Although in this study there have not been taken current measurements, the reversal of the surface circulation after the presence of SW winds (up-fjord) had been previously noted in Vestfjorden (Furnes and Sundby, 1981) and in Svalbard fjords (Skarðhamar and Svendsen, 2010). Moreover, in the survey carried out by Furnes and Sundby (1981), it was noted that the reversal of the surface circulation caused a deep Atlantic Water outflow. The previous observations (Furnes and Sundby, 1981) and the downward slope of the pycnocline towards the head of the fjord (figure 8) (Inall and Gillibrand, 2010), also observed in this study, allow to confirm that there was an AW deep outflow in Vestfjorden in 2014, 2015, April I on 2016 and March 2017. Mixing intensity may vary in different parts of the fjord, being in some parts more important than the freshwater runoff. This is noted on the surface salinities of 2017. Within a month, the inner part of the fjord (station 1, 2, 3, 4) got fresher whereas the outer stations were saltier than in March. Strong down-fjord winds enhanced the outflow of fresher water, therefore generating a compensating sub-surface current of water from the shelf as also found in other fjords (Cottier *et al.,* 2007; Nilsen *et al.,* 2008; Cottier *et al.,* 2010). This could explain the stronger coastal influence at the outer stations in April 2017, since in the week prior the cruise the dominant winds were in down-fjord direction. The general freshening and warming of the surface through spring, with the latest cruises showing more summer-like characteristics, suggests that Vestfjorden is in a process of shifting from the spring profile to summer profile in April.

5.1.2 Eddies and fronts in Vestfjorden

Fjord hydrography is affected by its topography (Inall and Gillibrand, 2010). In Vestfjorden, this becomes evident by some special oceanographic features related to a decrease in depth around 68.1 ºN. These features are the formation of a cyclonic eddy or a front, which can be seen in the temperature, salinity, and density plots (figure, 6, 7, 8).

Short-term variability (i.e., variations between days) could be observed in the years where more than one repeat of transect was taken. In 2016 and 2019 very short scale changes (i.e., days) in these hydrographic features could be observed, whereas data from 2017 allowed to see a longer time scale (still intra-seasonal) change (i.e., a month). The upper water column is affected by short-scale processes (Franks, 2014). The variations of the hydrographic features in the upper water layer can be noted in 2016. Strong SW winds piled up the water at the head of the fjord, probably forming a temperature and salinity front while interacting the NCW with the mixed coastal water (mNCW; colder and fresher) from inside the fjord. During the survey of Furnes and Sundby (1981), they found a front in the same position as in this study. In the period between April I and April II, the wind changed from S/SW winds (up-fjord) to NE winds (down-fjord) reinstating the estuarine circulation (Cottier *et al.*, 2007; Nilsen *et al.*, 2008; Cottier *et al.*, 2010), thus, likely pushing the front outwards towards the mouth of the fjord and causing a deepening of the pycnocline (Furnes and Sundby, 1981). Between April II and April III, there is a reduction of wind intensity, reducing in intensity the surface outflow. This, combined with the bottom topography, might be the cause of the formation of a cyclonic eddy around station 4. The formation of eddies in Vestfjorden is dependent to the baroclinic currents associated with the front (Mitchelson and Sundby, 2001). Thus, the restrictions on the flow of the freshwater runoff and the NCC will determine the positions of the eddies. The eddy will stay in the fjord during periods of calm conditions (Mitchelson and Sundby, 2001). In 2019, the spatial coverage of April II and April III, is not optimal, since just stations 2, 3, 4 and 1, 2, 3 were taken respectively. In April I, there is the presence of another cyclonic eddy in the same place as in April III of 2016. As opposite of 2016, the wind pattern before the April I in 2019 does not show a calm condition pattern. Actually, the wind prior the cruise in April I 2019 is very chaotic, following no common pattern. Taking this with some scepticism (due to limited spatial coverage), it looks like the eddy is moving into the fjord. This, and as proposed before, might be due to a higher penetration of the NCC into the fjord.

5.2 Phytoplankton distribution and its relations with hydrography.

5.2.1 Common phytoplankton distribution in Vestfjorden during spring

The biomass of phytoplankton below 50 m is near zero in all years probably due lack of light, hindering photosynthesis (figure 9). In contrast, the nutrient concentrations below 50 m increased a lot which shows that deeper from there, phytoplankton could not grow, and was not using nutrients. In addition to the vertical structure, the horizontal phytoplankton distribution varied a lot in the years of the present study since the spring bloom is a short time scale process and the cruises were not happening on the same date. Also, the spring bloom has been found to vary in intensity and timing in Northern Norway fjords (Reigstad and Wassmann, 1996; Wassmann *et al.*, 1996).

The years investigated here can be grouped into two groups: In some years in which a bloom has been observed during the sampling, and in some years where only a weakly elevated fluorescence has been found. The years with the only weakly elevated fluorescence signal are 2014 and 2017 (both March and April) The fluorescence on the non-bloom situation was similar to the results obtained by Wassmann *et al.*, (2000) in Balsfjord during spring. There could be different reasons for the weak fluorescence signal: Either the bloom was not triggered yet or the bloom already occurred. In March, nutrient concentrations were found to be higher than the other years, but in the surface are already lower than the bottom layer. This could indicate that, even if the bloom did not occur yet, a weak algal growth has already happened. In Balsfjord, as well as in other northern Norwegian fjords, the start of the spring bloom varies between the years (Reigstad and Wassmann, 1996; Wassmann *et al.*, 1996). The starting of the bloom in Balsfjord was observed in March (Eilertsen and Taasen, 1984) and April (Wassmann *et al.*, 2000). The high nutrient concentrations in the upper water column (first 50 m) in Vestfjorden in March 2017 may suggest that the fjord was in a pre-bloom situation. The late time of spring in which the sampling was done for 2014 and April 2017, would suggest that the bloom had already happened in Vestfjorden. Unfortunately, there are no nutrient data for these years available, which could confirm that the surface layer was strongly nutrient depleted. However, in April 2017 the chl *a*/phaeophytin ratio was 10 times smaller than in March 2017 (data not shown; mainfile cruise 2017). This indicates a higher percentage of degraded (older) material, which suggests that the bloom was in a decreasing phase. The year 2017 is most likely to be a post-bloom situation, but nutrient data would be necessary to confirm that. And as the sampling

in 2014 took place at approximately the same time as in 2017, it is assumed that also in 2014 a post bloom stage was reached.

The position and intensity of the chlorophyll *a* peak varied between the years in which the bloom was occurring. Fluorescence distribution was noted to vary a lot in surface waters indicating a patchy distribution of the phytoplankton (Wassmann *et al.,* 2000). In 2015, the bloom was most likely in its exponential growth phase, since fluorescence are very high (although lower that the fluorescence signal in Balsfjord (Eilertsen and Taasen, 1984) and the surface is still not nutrient depleted (figure, 10, 11, 12). The lowest concentration of nutrients was observed in station 4 and station 5, which suggests either that the bloom was initiated there and that the phytoplankton has been growing there for more time (and used up nutrients), or that the phytoplankton has somehow been using up nutrients faster in the middle fjord. Since the spring bloom starts before further south, it can be advected into Vestfjorden as well as it happens with zooplankton (Espinasse *et al.,* 2016).

5.2.2 Influence of hydrography and hydrographic features on the phytoplankton distribution

The fluorescence in the mixed layer has not an even vertical distribution and also showed a horizontal variability. To understand this patchy distribution and the development of the spring bloom it is important to understand the hydrographical drivers. Most important is here the restratification of the water column after winter (Mahadevan *et al.,* 2012) and the upwelling of nutrient and phytoplankton from deeper layers (Mahadevan, 2016). Higher fluorescence was in present study observed in the middle of Vestfjorden (station 4) than at its mouth. This does not mean that the bloom did only occur just there, or in a lower intensity, but means there is a delaying on the start of the bloom in the inner-most and outer-most part of the fjords. In the Norwegian Sea, the spring bloom occurs first in the Coastal Waters (i.e., NCW) and later in AW and Arctic Waters (Rey, 2004 in Brom and Melle, 2007). As shown in section 5.1.1, from the middle fjord to the outside, there surface water mass can be defined as the NCW. But from the middle (station 4) to the inside, the surface water mass will represent a mixed coastal water (mNCW), being colder and fresher than the NCW. Thus, mNCW has more “Arctic-alike” characteristics therefore explaining the delaying of the bloom in the inner fjord.

The pattern shown for 2015 with lower nutrient concentration for the middle stations (station 4 and station 5) is repeated in all the cruises in which the bloom was happening. This, as explained before, can suggest that the bloom was initiated there in the middle of Vestfjorden, which is

rather uncommon, because it is usually assumed that the bloom starts in regions of with little water column mixing. However, around the stations 4 and 5, fronts or eddies were also commonly observed (figure 6, 7, 8). When the turbulent mixing was shut-down by frontal stratification, the turbulent mixing may become smaller than the Critical Turbulence (Huisman *et al.,* 1999) and the bloom can develop (Taylor and Ferrari, 2011b). Also, the presence of shallow mixed layers caused by the formation of eddies, can allow the bloom to develop (Mahadevan *et al.,* 2012). Apart from that, the presence of an oceanic front allows the nutrients from the deeper layers to the surface layer, thus maintaining the growth of phytoplankton. Further, the link between the phytoplankton maximum and the front/eddy was clearly shown in 2016. In April I, the maximum abundance of phytoplankton is associated to the front in the middle of Vestfjorden. When the wind changed the front was pushed outwards, and the fluorescence signal in the middle of the fjord decreased, but it increased in the outer most part of Vestfjorden where the front was then found. As the wind relaxed, the formation of a cyclonic eddy in the middle fjord produced an increase of the biomass of phytoplankton on a subsurface fluorescence maximum (20-25 m). The highest vertical velocities during the formation of a mixed layer eddy are usually at around half of the depth of the mixed layer depth (Mahadevan, 2016). The fluorescence maximum in April III was actually at around that depth, potentially indicating the place with highest upward nutrient flux from greater, nutrient rich depth. The presence of a subsurface maximum indicates nutrient limitation in the surface layer, which indicated that the bloom was in a later phase (Lutter *et al.,* 1989). All these observationswould match the theory of the formation of shallow mixed layers by the presence of cyclonic eddies (Mahadevan *et al.,* 2012), the shutdown of vertical mixing by oceanic fronts (Taylor and Ferrari, 2011b) and the upwelling caused by the hydropgraphic features.

This same phenomenon could also be observed in 2018, but weaker both in the strength of the front and the fluorescence signal, and in 2019, when the presence of a cyclonic eddy led to an interesting phytoplankton biomass distribution. In the centre of the eddy, there was a subsurface fluorescence maximum, indicating that the bloom there was in its peak (Lutter *et al.,* 1989). At both sides of the eddy, and probably related to the upwelling generated to the front associated to it, the bloom grows up to the surface. This may also indicate that the bloom at both sides of the eddy was in an initial phase (Eilertsen and Taasen, 1984; Lutter *et al.,*1989). The cruises in 2016, 2018, and 2019 happened earlier in April than the cruise in 2015, and thus the bloom was in exponential phase. This can indicate the following development of the spring bloom in Vestfjorden:

(1) After the bloom is induced by the influence of a hydrographic feature in the middle fjord, it will be a second bloom (or the first bloom will spread) along the whole fjord.

(2) If there is not a formation of such hydrographic feature (front/eddy) in the middle fjord, the onset of the bloom will be delayed until this feature conditions are given or some certain hydrographic conditions are reached.

The subsurface fluorescence maximum in the centre of the eddy in 2019 may support the scenario 1 since the bloom at both sides of was at an earlier stage of development. Scenario 2 is based on the observations of 2015. Probably, the high winds prior the cruise in 2015 kept the turbulent mixing active longer through spring and inhibited the displacement of the frontal stratification (Chiswell, 2013). This may have resulted in an inhibition of the formation of shallow mixed layers in the middle fjords, and therefore a delay the initiation of the spring bloom until the water column presented the conditions needed for phytoplankton to grow. Therefore, I can suggest, that a possible mechanism for the bloom formation in Vestfjorden is dependant of the presence of the formation of a hydrographic feature in the middle fjord, and from there will spread inwards and outwards. If such feature is not formed, the bloom initiation will be delayed until the water column reaches certain background conditions.

Overall, I can state that the distribution on phytoplankton in Vestfjorden is affected by hydrography. The different characteristics of the water masses (either NCW or mNCW), will determine the timing of the bloom, initiating before in NCW influenced areas. As well, hydrographic features seem to have a huge importance in the spring bloom development in Vestfjorden by enhancing the upward nutrient flux that can enhance the phytoplankton growth. Since in NCW influenced areas have an earlier development of the spring bloom (Rey *et al.*, 2004), the advection of phytoplankton rich waters into the fjord and its posterior upwelling by the presence of a front/eddy, might be a mechanism be the reason of the earlier onset of the spring bloom if compared with Balsfjord. The data suggests that the formation of hydrographic features were important for the bloom development and this may also be the case for other fjords. However, the data on this study is not strong enough to confirm this suggestions, so further research must be carried out with measures of turbulence, and longer temporal coverage during spring and other times of the year.

6 Conclusion

The water column in Vestfjorden in spring is stratified. The surface gets warmer and fresher as it is getting closer to summer while the warmer and saltier bottom layer stays rather constant. The strong thermal stratification in 2018, and the stratified water column in march suggests that Vestfjorden stays stratified thorough the whole year, having no periods in which the water column is fully mixed. Even if the effect of the earth rotation is important in Vestfjorden, the presence of a cross-fjord (from head to mouth) temperature gradient indicates the presence of Estuarine circulation. The wind affects greatly the estuarine circulation in the fjord, causing its inversion after short periods of down-fjord winds (NE). The presence of hydrographic features such as eddies and fronts is common Vestfjorden. The position and formation of the hydrographic features will also be affected by the wind and the position and strength of the NCC. Nutrient concentration increased from 50 m indicating no phytoplankton growth. The fluorescence in Vestfjorden in spring varies in intensity and spatial distribution during the years of the study. The data suggest that the bloom can develop in the middle fjord, possibly advected from regions further south where the bloom started earlier. The bloom initiation may be linked to the development of a hydrographic feature in the middle part of the fjord, allowing the formation of shallow mixed layers for the phytoplankton to grow, and the upwelling of nutrient rich waters. The phytoplankton seems to be strongly linked to the hydrographic features, as shown on the survey in 2016, where the maximum fluorescence peak apparently followed the front in the fjord and the formation of an eddy.

7 References

Albretsen, J., Aure, J., Sætre, R., & Danielssen, D. S. (2012). Climatic variability in the Skagerrak and coastal waters of Norway. *ICES Journal of Marine Science*, *69*(5), 758-763.

Bech, P. A. (1982). *Planteplankton og primærproduksjon i Balsfjorden og Tromsøysundet, 1980. Cand. Real* (Doctoral dissertation, thesis, University of Tromsø).

Behrenfeld, M. J. (2010). Abandoning Sverdrup's critical depth hypothesis on phytoplankton blooms. *Ecology*, *91*(4), 977-989.

Boccaletti, G., Ferrari, R., & Fox-Kemper, B. (2007). Mixed layer instabilities and restratification. *Journal of Physical Oceanography*, *37*(9), 2228-2250.

Bristow, L. A., Mohr, W., Ahmerkamp, S., & Kuypers, M. M. (2017). Nutrients that limit growth in the ocean. *Current Biology*, *27*(11), R474-R478.

Brody, S. R., & Lozier, M. S. (2014). Changes in dominant mixing length scales as a driver of subpolar phytoplankton bloom initiation in the North Atlantic. *Geophysical Research Letters*, *41*(9), 3197-3203.

Brody, S. R., & Lozier, M. S. (2015). Characterizing upper-ocean mixing and its effect on the spring phytoplankton bloom with in situ data. *ICES Journal of Marine Science*, *72*(6), 1961-1970.

Broms, C., & Melle, W. (2007). Seasonal development of Calanus finmarchicus in relation to phytoplankton bloom dynamics in the Norwegian Sea. *Deep Sea Research Part II: Topical Studies in Oceanography*, *54*(23-26), 2760-2775.

Chiswell, S. M., Bradford‐Grieve, J., Hadfield, M. G., & Kennan, S. C. (2013). Climatology of surface chlorophyll a, autumn‐winter and spring blooms in the southwest Pacific Ocean. *Journal of Geophysical Research: Oceans*, *118*(2), 1003-1018.

Chiswell, S. M., Calil, P. H., & Boyd, P. W. (2015). Spring blooms and annual cycles of phytoplankton: a unified perspective. *Journal of Plankton Research*, *37*(3), 500-508.

Cole, H. S., Henson, S., Martin, A. P., & Yool, A. (2015). Basin-wide mechanisms for spring bloom initiation: how typical is the North Atlantic? *ICES Journal of Marine Science*, *72*(6), 2029-2040.

Cottier, F. R., Nilsen, F., Inall, M. E., Gerland, S., Tverberg, V., & Svendsen, H. (2007). Wintertime warming of an Arctic shelf in response to large‐scale atmospheric circulation. *Geophysical Research Letters*, *34*(10).

Cottier, F. R., Nilsen, F., Skogseth, R., Tverberg, V., Skarðhamar, J., & Svendsen, H. (2010). Arctic fjords: a review of the oceanographic environment and dominant physical processes. *Geological Society, London, Special Publications*, *344*(1), 35-50.

Degerlund, M., & Eilertsen, H. C. (2010). Main species characteristics of phytoplankton spring blooms in NE Atlantic and Arctic waters (68–80 N). *Estuaries and coasts*, *33*(2), 242-269.

Eggvin, J. (1931). Litt om Vestfjordens vannmasser i skreitiden. *Arsberetning vedkommenderende Norges Fiskerier*, *2*, 97-100. (in Norwegian)

Eilertsen, H. C., & Taasen, J. P. (1984). Investigations on the plankton community of Balsfjorden, northern Norway. The phytoplankton 1976–1978. Environmental factors, dynamics of growth, and primary production. *Sarsia*, *69*(1), 1-15

Eilertsen, H. C., Falk-Petersen, S., Hopkins, C. C. E., & Tande, K. (1981). Ecological investigations on the plankton community of Balsfjorden, northern Norway: program for the project, study area, topography, and physical environment. *Sarsia*, *66*(1), 25-34.

Ellertsen, B., Fossum, P., Solemdal, P., Sundby, S., & Tilseth, S. (1987). The effect of biological and physical factors on the survival of Arcto-Norwegian cod and the influence on recruitment variability. *Proceedings of the third Soviet-Norwegian Symposium. Murmansk, 26-28 May 1986*

Ellertsen, H. C. (1993). Spring blooms and stratification. *Nature*, *363*(6424), 24-24

Espinasse, B., Tverberg, V., Basedow, S. L., Hattermann, T., Nøst, O. A., Albretsen, J., ... & Eiane, K. (2017). Mechanisms regulating inter‐annual variability in zooplankton advection over the Lofoten shelf, implications for cod larvae survival. *Fisheries Oceanography*, *26*(3), 299-315.

Farmer, D. M., & Freeland, H. J. (1983). The physical oceanography of fjords. *Progress in Oceanography*, *12*(2), 147-219.

Franks, P. J. (2014). Has Sverdrup's critical depth hypothesis been tested? Mixed layers vs. turbulent layers. *ICES Journal of Marine Science*, *72*(6), 1897-1907.

Furnes, G. K., & Sundby, S. (1981). Upwelling and wind induced circulation in Vestfjorden. *The Norwegian Coastal Current. R. Sætre and M. Mork (eds.)*, *1*, 152-177.

Gran, H. H., & Braarud, T. (1935). A quantitative study of the phytoplankton in the Bay of Fundy and the Gulf of Maine (including observations on hydrography, chemistry and turbidity). *Journal of the Biological Board of Canada*, *1*(5), 279-467.

Helland-Hansen, B., & Nansen, F. (1909). *The Norwegian Sea: its physical oceanography based upon the Norwegian researches 1900-1904*. Det Mallingske Bogtrykkeri.

Holm-Hansen, O., & Riemann, B. (1978). Chlorophyll a determination: improvements in methodology. *Oikos*, 438-447.

Huisman, J. E. F., van Oostveen, P., & Weissing, F. J. (1999). Critical depth and critical turbulence: two different mechanisms for the development of phytoplankton blooms. *Limnology and Oceanography*, *44*(7), 1781-1787.

Inall, M. E., & Gillibrand, P. A. (2010). The physics of mid-latitude fjords: a review. *Geological Society, London, Special Publications*, *344*(1), 17-33.

Ingvaldsen, R., Reitan, M. B., Svendsen, H., & Asplin, L. (2001). The upper layer circulation in Kongsfjorden and Krossfjorden-A complex fjord system on the west coast of Spitsbergen. *Memoirs of National Institute of Polar Research. Special issue, 393 - 407*

IOC, S. (2010). IAPSO: The international thermodynamic equation of seawater–2010: Calculation and use of thermodynamic properties, Intergovernmental Oceanographic Commission, Manuals and Guides No. 56. *UNESCO, Manuals and Guides*, *56*, 1-196.

Jones, B., Boudjelas, S., & Mitchelson‐Jacob, E. G. (1997). Topographic steering of winds in Vestfjorden, Norway. *Weather*, *52*(10), 304-311.

Klinck, J. M., O'Brien, J. J., & Svendsen, H. (1981). A simple model of fjord and coastal circulation interaction. *Journal of Physical Oceanography*, *11*(12), 1612-1626.

Mahadevan, A. (2016). The impact of submesoscale physics on primary productivity of plankton. *Annual review of marine science*, *8*, 161-184.

Mahadevan, A., & Archer, D. (2000). Modeling the impact of fronts and mesoscale circulation on the nutrient supply and biogeochemistry of the upper ocean. *Journal of Geophysical Research: Oceans*, *105*(C1), 1209-1225.

Mahadevan, A., D'Asaro, E., Lee, C., & Perry, M. J. (2012). Eddy-driven stratification initiates North Atlantic spring phytoplankton blooms. *Science*, *337*(6090), 54-58.

Mitchelson-Jacob, G., & Sundby, S. (2001). Eddies of Vestfjorden, Norway. *Continental Shelf Research*, *21*(16-17), 1901-1918.

Mork, K. A., Skagseth, Ø., & Søiland, H. (2019). Recent warming and freshening of the Norwegian Sea observed by Argo data. *Journal of Climate*, *32*(12), 3695-3705.

Nilsen, F., Cottier, F., Skogseth, R., & Mattsson, S. (2008). Fjord–shelf exchanges controlled by ice and brine production: the interannual variation of Atlantic Water in Isfjorden, Svalbard. *Continental Shelf Research*, *28*(14), 1838-1853.

Nilsen, F., Gjevik, B., & Schauer, U. (2006). Cooling of the West Spitsbergen Current: Isopycnal diffusion by topographic vorticity waves. *Journal of Geophysical Research: Oceans*, *111*(C8).

Nordby, E., Tande, K. S., Svendsen, H., Slagstad, D., & Båmstedt, U. (1999). Oceanography and fluorescence at the shelf break off the north Norwegian coast (69°′ N-70° 30′ N) during the main productive period in 1994. *Sarsia*, *84*(3-4), 175-189.

Lutter, S., Taasen, J. P., Hopkins, C. C. E., & Smetacek, V. (1989). Phytoplankton dynamics and sedimentation processes during spring and summer in Balsfjord, northern Norway. *Polar Biology*, *10*(2), 113-124.

Ottersen, G., Bogstad, B., Yaragina, N., Stige, L. C., Vikebø, F., & Dalpadado, P. (2013) A review of early life history dynamics of Barents Sea cod. *ICES Journal of Marine Science (2014), 71(8), 2064–2087*.

Pavlov, A. K., Tverberg, V., Ivanov, B. V., Nilsen, F., Falk-Petersen, S., & Granskog, M. A. (2013). Warming of Atlantic Water in two west Spitsbergen fjords over the last century (1912–2009). *Polar Research, 32*(1), 11206.

Peng, T. H., Takahashi, T., Broecker, W. S., & Olafsson, J. O. N. (1987). Seasonal variability of carbon dioxide, nutrients and oxygen in the northern North Atlantic surface water: observations and a model. *Tellus B: Chemical and Physical Meteorology*, *39*(5), 439-458.

Reigstad, M., & Wassmann, P. (1996). Importance of advection for pelagic-benthic coupling in north Norwegian fjords. *Sarsia*, *80*(4), 245-257.

Rey, F. (2004). Phytoplankton, the grass of the sea. In: Skjoldal, H. R., & Saetre, R. (Eds.). (2004). *The Norwegian sea ecosystem*. Akademika Pub.

Sætre, R. (1999). Features of the central Norwegian shelf circulation. *Continental Shelf Research, 19*(14), 1809-1831.

Sætre, R. (Ed.). (2007). *The Norwegian coastal current: oceanography and climate*. Akademika Pub.

Siegel, D. A., McGillicuddy Jr, D. J., & Fields, E. A. (1999). Mesoscale eddies, satellite altimetry, and new production in the Sargasso Sea. *Journal of Geophysical Research: Oceans, 104*(C6), 13359-13379.

Skarðhamar, J., & Svendsen, H. (2010). Short-term hydrographic variability in a stratified Arctic fjord. *Geological Society, London, Special Publications*, *344*(1), 51-60.

Skogseth, R., Sandvik, A. D., & Asplin, L. (2007). Wind and tidal forcing on the meso-scale circulation in Storfjorden, Svalbard. *Continental Shelf Research*, *27*(2), 208-227.

Stedmon, C., 2020. Personal communication. Lecture on nutrients on the course “Chemical Oceanography in the Arctic” UNIS Svalbard.

Sundby, S. (1978). In/out-flow of coastal water in Vestfjorden. ICES. *Council Meeting of the International Council for the Exploration of the Sea, 1978/C: 51, 17 pp. (Mimeo.)*

Sundby, S. (1984). Influence of bottom topography on the circulation at the continental shelf off northern Norway. *Fiskeridirektoratets Skrif ter Serie Havundersokelser 7. 501-519.. 17. 501-519,*

Svendsen, H., Beszczynska-Møller, A., Hagen, J. O., Lefauconnier, B., Tverberg, V., Gerland, S., & Azzolini, R. (2002). The physical environment of Kongsfjorden–Krossfjorden, an Arctic fjord system in Svalbard. *Polar Research*, *21*(1), 133-166.

Sverdrup, H. U. (1953). On conditions for the vernal blooming of phytoplankton. *Journal du Conseil / Conseil Permanent International pour l'Exploration de la Mer* , *18*(3), 287-295.

Syvitski, J.P.M., Burrell, D.C., and Skei, J.M., (2012). Fjords: Processes and Products. *Springer Science & Business Media*. ISBN: 978-1-4612-4632-9

Takahashi, T., Olafsson, J., Goddard, J. G., Chipman, D. W., & Sutherland, S. C. (1993). Seasonal variation of CO2 and nutrients in the high - latitude surface oceans: A comparative study. *Global Biogeochemical Cycles*, *7*(4), 843-878

Taylor, J. R., & Ferrari, R. (2011a). Shutdown of turbulent convection as a new criterion for the onset of spring phytoplankton blooms. *Limnology and Oceanography*, *56*(6), 2293-2307.

Taylor, J. R., & Ferrari, R. (2011b). Ocean fronts trigger high latitude phytoplankton blooms. *Geophysical Research Letters*, *38*(23).

Townsend, D. W., Keller, M. D., Sieracki, M. E., & Ackleson, S. G. (1992). Spring phytoplankton blooms in the absence of vertical water column stratification. *Nature*, *360*(6399), 59.

Wassmann, P., Reigstad, M., Øygarden, S., & Rey, F. (2000). Seasonal variation in hydrography, nutrients, and suspended biomass in a subarctic fjord: applying hydrographic features and biological markers to trace water masses and circulation significant for phytoplankton production. *Sarsia*, *85*(3), 237-249.

Wassmann, P., Svendsen, H., Keck, A., & Reigstad, M. (1996). Selected aspects of the physical oceanography and particle fluxes in fjords of northern Norway. *Journal of Marine Systems*, *8*(1-2), 53-71.